Biosensors and Bioelectronics 80 (2016) 273–287

Contents lists available at ScienceDirect

Biosensors and Bioelectronics

journal homepage: www.elsevier.com/locate/bios

Nano-biosensors to detect beta-amyloid for Alzheimer's disease management

Ajeet Kaushik*, Rahul Dev Jayant, Sneham Tiwari, Arti Vashist, Madhavan Nair*

Center for Personalized Nanomedicine, Institute of Neuro immune Pharmacology, Department of Immunology, Herbert Wertheim College of Medicine, Florida International University, Miami, FL, USA

ARTICLE INFO

Article history:
Received 22 December 2015
Received in revised form
21 January 2016
Accepted 27 January 2016
Available online 28 January 2016

Keywords:
Beta-amyloid
Alzheimer's diseases
Diseases management
Electrochemical sensor
Point-of-care sensing

ABSTRACT

Beta-amyloid (β-A) peptides are potential biomarkers to monitor Alzheimer's diseases (AD) for diagnostic purposes. Increased β-A level is neurotoxic and induces oxidative stress in brain resulting in neurodegeneration and causes dementia. As of now, no sensitive and inexpensive method is available for β-A detection under physiological and pathological conditions. Although, available methods such as neuroimaging, enzyme-linked immunosorbent assay (ELISA), and polymerase chain reaction (PCR) detect β-A, but they are not yet extended at point-of-care (POC) due to sophisticated equipments, need of high expertize, complicated operations, and challenge of low detection limit. Recently, β-A antibody based electrochemical immuno-sensing approach has been explored to detect β-A at pM levels within 30–40 min compared to 6–8 h of ELISA test. The introduction of nano-enabling electrochemical sensing technology could enable rapid detection of β-A at POC and may facilitate fast personalized health care delivery. This review explores recent advancements in nano-enabling electrochemical β-A sensing technologies towards POC application to AD management. These analytical tools can serve as an analytical tool for AD management program to obtain bio-informatics needed to optimize therapeutics for neurodegenerative diseases diagnosis management.

Contents

1. Introduction: Alzheimer's diseases and challenges

Alzheimer's disease (AD) is an irreversible progressive brain disorder (Mount and Downton, 2006). It causes severe impairment to memory and cognitive function, which leads to behavioral and psychological symptoms such as depression, stress, anxiety and mood disturbances (Claeysen et al., 2015). World health organization (WHO) declared AD as a worldwide socio-economic concern of over $600 billion cost. WHO confirms 37 million people affected by dementia and 17 million of them are affected by AD. Recent studies confirm that steady increment in AD incidence especially in aging population would be over 3-fold by 2050 (Fig. 1) (Mount and Downton, 2006).

The risk factors of AD associated with aged population are very serious with no available cure. Therefore, continuous monitoring of AD progress becomes essential for a patient to select therapeutics and manage disease (Haes et al., 2005; Kurapati et al.,

* Corresponding authors.
E-mail addresses: ajeet.npl@gmail.com (A. Kaushik), nairm@fiu.edu (M. Nair).

http://dx.doi.org/10.1016/j.bios.2016.01.065
0956-5663/

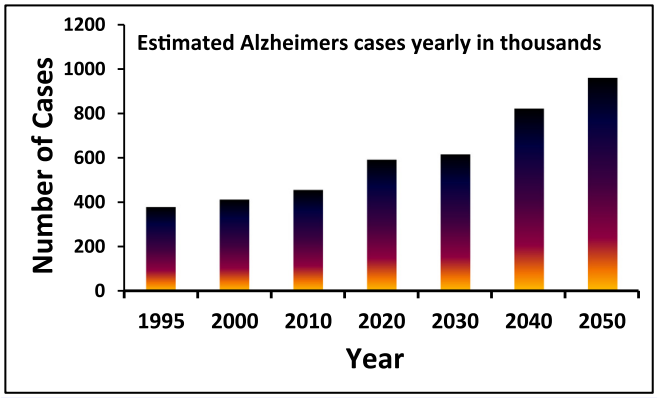

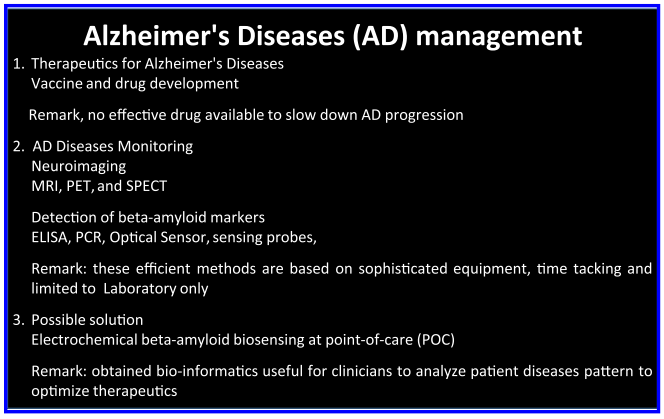

Fig. 1. Illustration of early estimated AD cases along with the approach and need of AD management.

2014; Rushworth et al., 2014; Shapshak et al., 2008). Available and approved drugs and therapies from food and drug administration (FDA) are not very effective and do not even slow down the AD progression. Thus developing novel strategies to monitor AD progression is of great significance for diagnostic, therapeutic significance and management of AD (Laske et al., 2015; Mosconi et al., 2007; Nestor et al., 2004; Sjögren et al., 2003).

More extremely, AD population is increasing in patients affected with other deadly infectious diseases such as human immunodeficiency virus (HIV), cancer, and Parkinson's. Synergistically, both AD and other infectious dementias cause severe impairments and still remains incurable (Adle-Biassette et al., 1995; András and Toborek, 2013; Green et al., 2005; Simioni et al., 2010). Recent discovery established a correlation between gene function, expression, structure, function of human genome between pathogenesis of infectious diseases and AD dementia disorders (András and Toborek, 2013; Kurapati et al., 2014; Shapshak et al., 2008; Simioni et al., 2010). We believe that due to availability of potential therapeutics such as antiretroviral therapy (ARV) therapy, anti-cancer drugs, and diseased management, patients have longer life and especially elderly patients have maximum probability of AD dementia. Thus monitoring of AD is crucial for timely diagnosis and treatment (Fig. 1). Clinical studies suggested that AD brain and traumatic brain injury exhibit similarities between accumulation of amyloid peptides mainly beta-amyloid (β-A) and tau protein (Tsitsopoulos and Marklund, 2013). To monitor AD in real samples such as interstitial fluid (ISF) and cerebrospinal fluid (CSF), both tau protein and β-A have served as potential biomarkers (Kolarova et al., 2012; Martić et al., 2012a; Martić et al., 2012b; Martic et al., 2013; Rains et al., 2013; Tsitsopoulos and Marklund, 2013). To make presented review well-focused and comprehensive, we highlight exclusively β-A as a potential biomarker for AD detection using nano-enabling biosensors. The detection and monitoring of β-A may prove as a potential way to monitor AD diseases.

2. Hypothesis of β-A to monitor Alzheimer's diseases

The role of β-A peptide for AD monitoring has been investigated and well-accepted (Claeysen et al., 2015; Haass and Selkoe, 2007; LaFerla et al., 2007). The β-A peptide exists in multiple assembly states such as monomers, oligomers, protofibrils, and fibrils (Fig. 2) (LaFerla et al., 2007). All the forms of β-A have various significant physiological or pathophysiological effects on AD progression. The monomer form of β-A is not neurotoxic while the oligomers and fibrils formed via nucleation-dependent complex process exhibit neurotoxicity and block long-term potentiation to affect synaptic plasticity. In general, AD dementia generates due to tangles of neurofibrils that consist of phosphorylated tau protein, β-A plaques and aggregation of insoluble hydrophobic β-A peptide (Butterfield et al., 2001; Hamley, 2012; Verdile et al., 2004; Xu et al., 2015). Degradation of transmembrane precursor; amyloid precursor protein (APP) leads towards β-A plaques formation. APP degradation takes place via two mechanisms namely amyloidogenic and non amyloidogenic pathways (Fig. 3) (Claeysen et al., 2015). First is Amyloidogenic mechanism which produces β-A peptide via cleaving APP by β-secretase i.e. beta-Site APP-cleaving enzyme (1BACE1) and γ-secretases. The β-A peptides produced through this manner form toxic oligomeric species and lead to plaque formation via aggregation. In second pathway, the cleavage of APP takes place via α-secretase i.e. a disintegrin and metalloproteinase domain-containing protein 10 (ADAM10) in neurons situated within β-A sequence. This

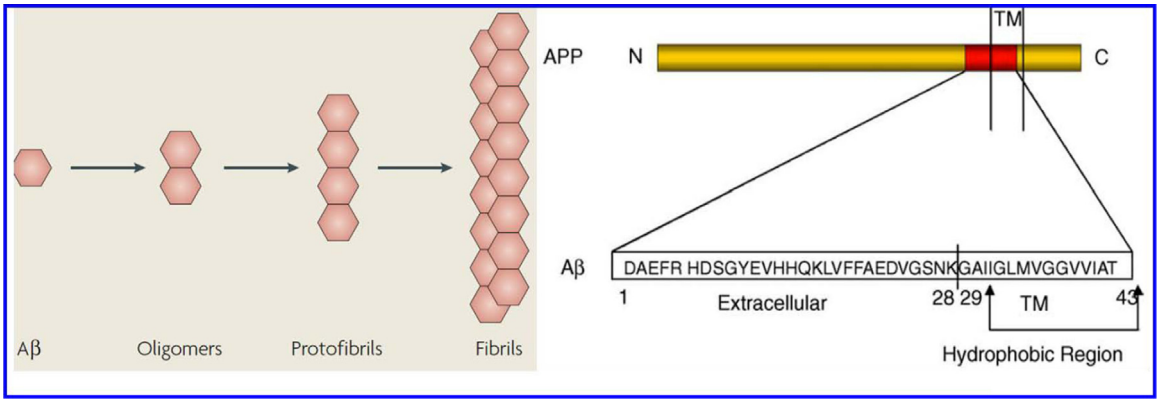

Fig. 2. Various forms of β-A form associated with AD progression. (Figure reprinted ref LaFeral et al., 2007, Copyright Nature-2007 and ref Verdile et al., 2004, Copyright Elsevier-2004.)

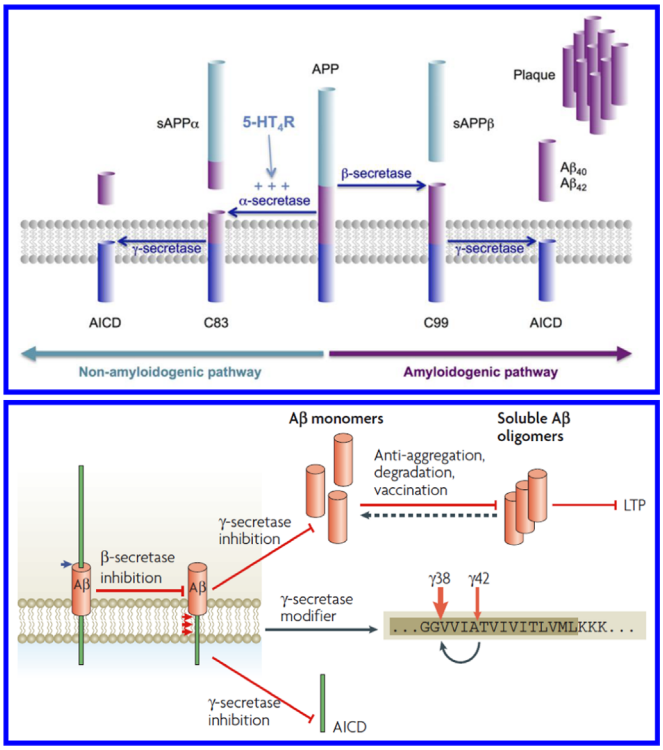

Fig. 3. Therapeutic approaches targeting β-A protein production and oligomerization. (Figure reprinted ref Claeysen et al., 2015, Copyright ACS-2015 and ref Haass et al., 2007, Copyright Nature-2007.)

mechanism stops the formation of the β-A and prevents the release of soluble secreted amyloid precursor protein-α (sAPPα) fragment. These alterations affect the neurotrophic and neuroprotective properties of the brain.

The plaque formation by β-A is associated with onset and AD progression. Two major isoforms of different amino acid chain length namely β-A_{1-40} and β-A_{1-42} are major contributory components for neurotic plaques fabrication (Kumar et al., 2014; Veloso et al., 2014). These two amyloid peptides exhibit differential rates of spontaneous self-association into supramolecular assemblies forming fibrils and plaques (Kumar et al., 2014). In brain, β-A_{1-40} is found in higher quantities than β-A_{1-42}. Plaque formation associated with β-A_{1-42} shows faster aggregation which causes more free radical damage leading to neurotoxicity. The β-A aggregation alters immunological response in the brain via affecting secretion of pro-inflammatory cytokines, formation of soluble neurotoxic oligomers and aggregating fibrils leading to severe dementia. The β-A oligomers incorporates with lipid bilayer of neuronal cells affecting cell membrane homeostatis, Ca+ ion up-regulation, membrane depolarization, reactive ion oxygen (ROS) enhancement, resulting in neurotransmitter excitotoxicity and neuronal cells death (Veloso et al., 2014; Wolfe, 2001).

Recently, efforts have been made to develop therapeutic strategies to reduce β-A burden via detection and inhibition of β-A production to explore potential therapeutics against AD. With respect to the stated context, State-of-the-art of β-A detection using qualitative and quantitative analytical tools to monitor β-A plaque formation to analyze AD progression monitoring is discussed critically in next section.

3. State-of-the-art of β-A detection

Conventional techniques to diagnose AD include post-mortem examination of patient brain via identification of senile plaques and neurofibrillary tangles (Beduer et al., 2015; Butterfield et al., 2001; Csernansky et al., 2005; Georganopoulou et al., 2005; Haes et al., 2005, 2004; Laske et al., 2015; Raymond et al., 2008; Rushworth et al., 2014; Sehgal et al., 2012; Shaw et al., 2009; Sjögren et al., 2003; Veloso et al., 2014; Verdile et al., 2004). AD diagnosis is based on clinical history and *in-vivo* brain imaging using magnetic resonance imaging (MRI) (Raymond et al., 2008), single-photon emission computed tomography (SPECT), metabolic positron emission tomography (PET) (Laske et al., 2015; Nestor et al., 2004; Viola et al., 2015), near infrared (NIR) responsive imaging (Zhang et al., 2013b), and surface plasma resonance imaging (SPRi) (Nestor et al., 2004). The neuropsychological, cognitive, and neurological tests are also in practice to analyze AD. Unfortunately, these methods are time consuming, expensive and with limited accuracy (~85%) (Georganopoulou et al., 2005). Recently, soluble markers for AD detection are also explored for disease monitoring (Nestor et al., 2004) like total tau protein or β-A levels in CSF or plasma samples (Georganopoulou et al., 2005).

Neuroimaging is a conventional and reliable qualitative technique for the assessment of AD in clinics. The techniques such as PET, MRI and NIR imaging are extensively adopted modalities for the detection of brain abnormalities due to AD. Various reviews have explained fundamentals, capabilities, and advancements of these methods to detect AD and their significance in clinical diagnosis. Significant efforts have been made to design and develop imaging and fluorescent agents with the capability to cross blood-brain-barrier (BBB) for neuroimaging of AD brain using appropriate methods (Fonseca-Santos et al., 2015). Unfortunately, no imaging method is well explored to diagnose AD brain of mice or human. Recent development in neuroimaging for β-A screening and detection for AD assessment are discussed briefly in this section.

Wadghiri et al. proposed transgenic mice as a suitable animal model for AD monitoring. On overexpression with mutant APP and presenilin-1 (APP/PS1), these mice developed β-A plaques similar to AD patients (Wadghiri et al., 2003). Authors used MRI to detect β-A plaques in transgenic mice brain using magnetically labeled β-A_{1-40} peptides having higher affinity with β-A (Fig. 4A). Magnetically labeled β-A_{1-40} particles injected via intra-arterial administration were able to cross BBB to bind with β-A plaques. The quantitative estimation of β-A plaques was performed using MRI scanning of immunohistochemistry. Presented *in-vitro* approach has significant scope to promote for real-time *in-vivo* AD monitoring at clinical level (Wadghiri et al., 2003). An ultrasound assisted delivery of an imaging fluorophore agent and anti β-A antibodies across BBB for AD detection was demonstrated by Raymond et al. (2008). Authors demonstrated delivery of Trypan blue, an amyloid staining red fluorophore, and anti-amyloid antibodies via intravenous administration in two different transgenic AD mouse strain (APPs: PSEN1dE9, PDAPP, 9–26 months). MRI guided AD monitoring and treatment was performed at hippocampus and exhibited 16.56 ± 5.4 fold increment in Trypan blue fluorescence intensity along with 2.76 ± 1.2 fold increment related to anti β-A antibodies localized to amyloid plaques. Authors proposed approaches as an imaging probe and pre-clinical drug screening methods, that can be used to deliver therapeutic cargos to AD brain (Raymond et al., 2008).

Near-infrared fluorescence (NIRF) based neuroimaging probes were investigated for AD monitoring and therapy at preclinical level. Fu et al., have explored various donor-acceptor near infrared (DANIR) probes based on different electron donor–acceptor end groups capable to interact through a π-conjugated system to detect β-A deposition in AD brain (Fu et al., 2015). Authors synthesized 2 probes of different chain length and excellent fluorescent properties (emission maxima > 650 nm and high quantum yields) which were capable to penetrate BBB and also wash out from

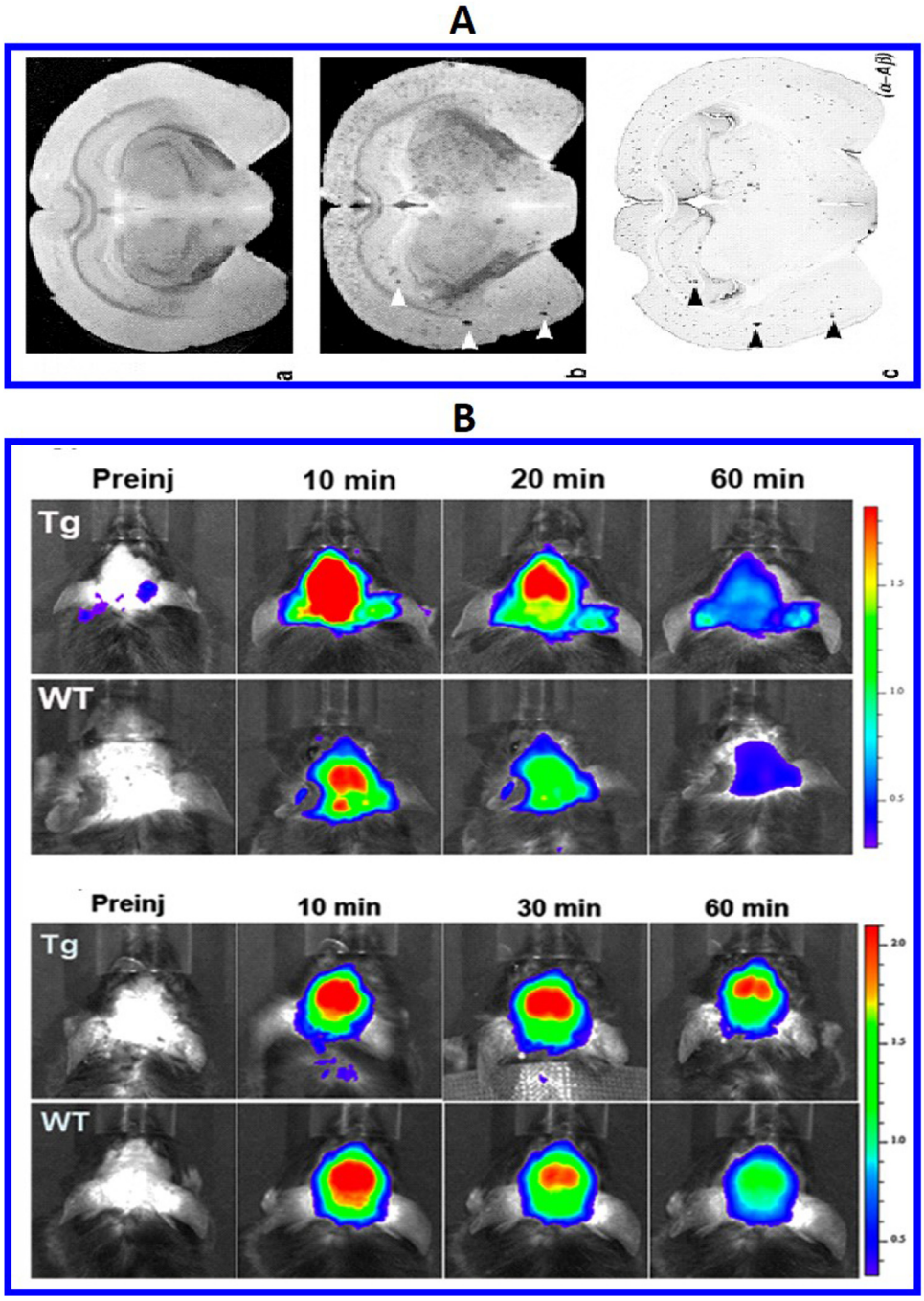

Fig. 4. (A) EX-vivo MRI for the detection of β-A after injection of Gd-DTPA-A_1–40 in (a) 6-month-old control, and (b) APP/PS1-transgenic mouse brains (Figure reprinted Ref Yousef Zaime Wadghiri, copyright Wiley InterScience-2013) (Wadghiri et al., 2003). These results were validated using immunohistochemistry (c). (B) In-vivo MRI imaged of 2 NIR responsive probes infected in mice to monitor β-A aggregation in mice as a function of time and imaging agents (Figure reprinted ref Hualong Fu, Copyright ACS-2015) (Fu et al., 2015).

brain. These probes exhibited high sensitivity, and high affinities to β-A aggregates (Kd = 8.8 nM and Kd = 1.9 nM). The results of *in-vivo* NIR imaging based on MRI showed that an optimized NIR probe can differentiate mouse model and can be used as a potential β-A neuroimaging probe for sensing β-A aggregation or plaques (Fu et al., 2015) (Fig. 4B). Recently, NIR neuroimaging probes were developed to monitor the β-A changes during therapy. Curcumin-based NIR fluorescence PET imaging probes have been investigated by Zhang et al., to detect β-A in both soluble and insoluble forms (Zhang et al., 2013b). Authors have designed (T-4)-[(1E,6E)-1,7-Bis[4-(dimethylamino)phenyl]-1,6-heptadiene-3,5-dionato-kO3,kO5]difluoroboron (CRANAD)-58 as NIR imaging probe. This probe showed significant change in fluorescence intensity on mixing with β-A species using *in-vitro* and *in-vivo* model. CRANAD-58 was sensitive to detect insoluble form of β-A plaques. This group also designed CRANAD-17, a curcumin scaffold to attenuate the cross-linking of $\beta\text{-A}_{1-42}$ induced by Cu ion via coordination with imidazoles on Histidine-13 and 14 (H13, H14) of β-A peptides (Zhang et al., 2013b).

Zhang et al. explored NIRF neuroimaging using CRANAD-3 to detect both form of β-A species in transgenic AD (APP/PS1) mice model (3–4 month old mice) (Fig. 5A) (Zhang et al., 2015). The

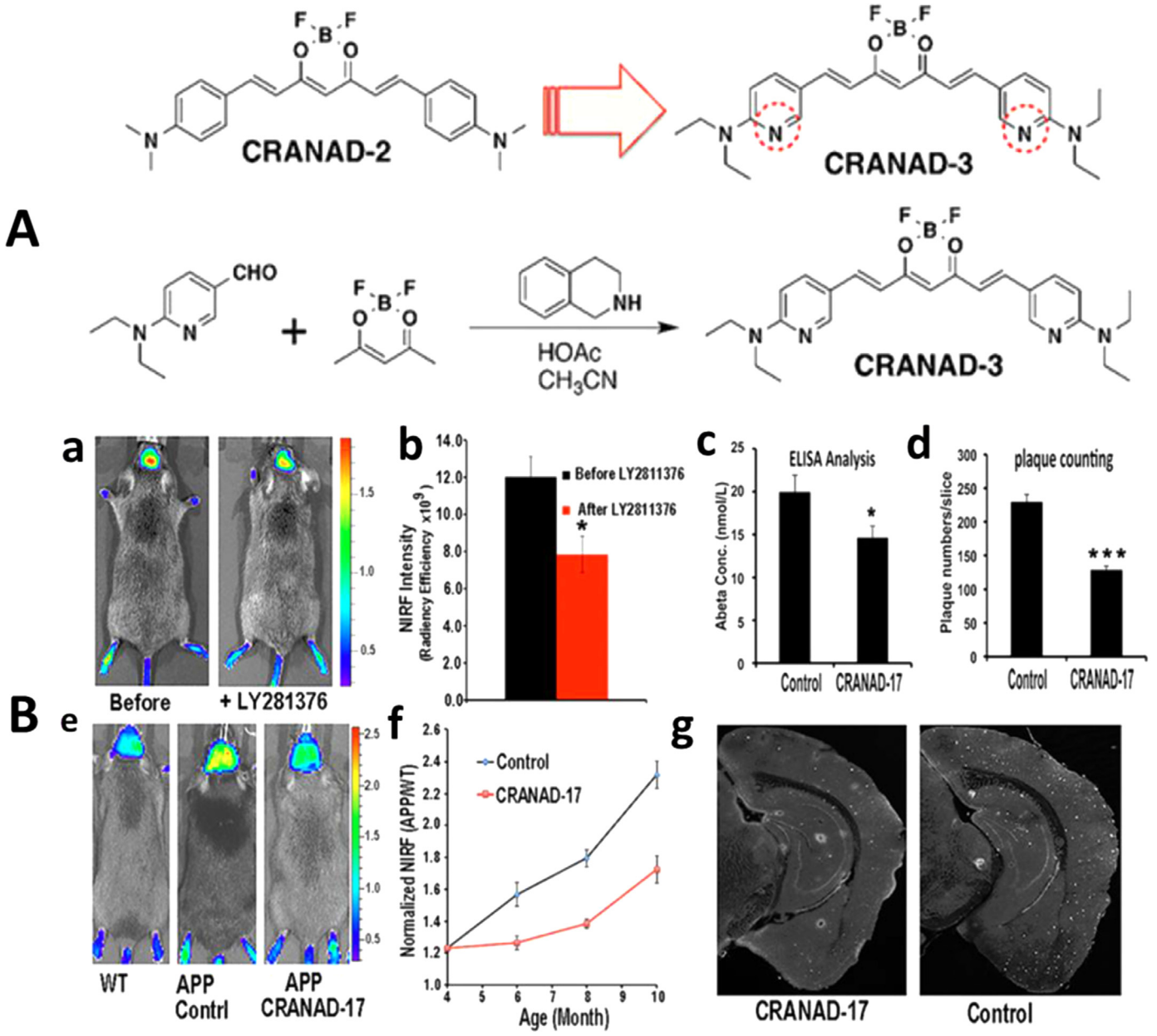

Fig. 5. (A) Chemical structure and synthesis of CRANAD-3 utilized as NIR responsive imaging agent. (B) Therapeutic effects of CRANAD-3 for AD monitoring, (a) Neuroimaging of APP/PS1 mice with CRANAD-3 before and after treatment with the BACE-1 inhibitor LY2811376 using in-vivo model with quantitative analysis (b), (c) NIRF images of 4-month APP/PS1 mice after 6 month of treatment with CRANAD-17 and their quantitative analysis (d), (e) validation of results using ELISA analysis, (f) plaque counting, and (g) histological staining with thioflavin S. (Figure Reprinted Ref. Xueli Zhang-2015, Copyright PNAAS or Science) (Zhang et al., 2015).

CRANAD-2 exhibited 2.29-fold higher signal in transgenic mice than wild-type mice of same age. This approach was successful to detect early stage AD. Authors also explored AD treatment monitoring in mice using β-A lowering drug i.e., LY281176, an amyloid cleaving enzyme-1 to treat AD affected mice (Fig. 5 B). The results confirmed that CRANAD-3 can be used to monitor reduction in β-A level during treatment validated by ELISA (Zhang et al., 2015).

A hydrophilic nano-vehicle (nanoparticles-IgG 4.1) was designed by Jaruszewski et al. to target cerebrovascular amyloid (CVA) for early diagnostics of AD (Jaruszewski et al., 2014). This developed nano-vehicle consists of dadolinium (Gd) based MRI or SPECT imaging contrast agents such as 125I and anti-inflammatory or anti-amyloidogenic agents such as curcumin or immunosuppressants such as dexamethasone to target and treat CVA. An anti-β-A antibody (IgG 4.1) was immobilized onto nano-vehicles for CVA deposits specific targeting. These developed therapeutic nano-vehicles effectively penetrated BBB and got uniformly distributed in brain. The MRI and SPECT imaging results confirmed that nano-vehicles can serve as effective diagnostic agents to detect and reduced CVA associated inflammation (Fig. 6) (Jaruszewski et al., 2014).

A new label/label-free silicon/silicon oxide (Si/SiO_2) microarray based immunoassay was developed by Gangi et al. to detect $\beta\text{-}A_{1-42}$ (Gagni et al., 2013). This platform functioned on the basis of interferometric reflectance imaging sensing and exhibited a high throughput leading to high sensitivity due to constructive interference (Fig. 7A). Authors coated Si/SiO_2 substrate using a ter-co-polymer [dimethylacrylamide (DMA), 3-(trimethoxysilyl)propyl methacrylate (MAPS) and N-Acryloyloxy succinimide (NAS)] and functionalized using anti-β-A antibody to bind with $\beta\text{-}A_{1-42}$ selectively for specific recognition using interferometric reflectance imaging sensor (IRIS). This method showed a detection limit of

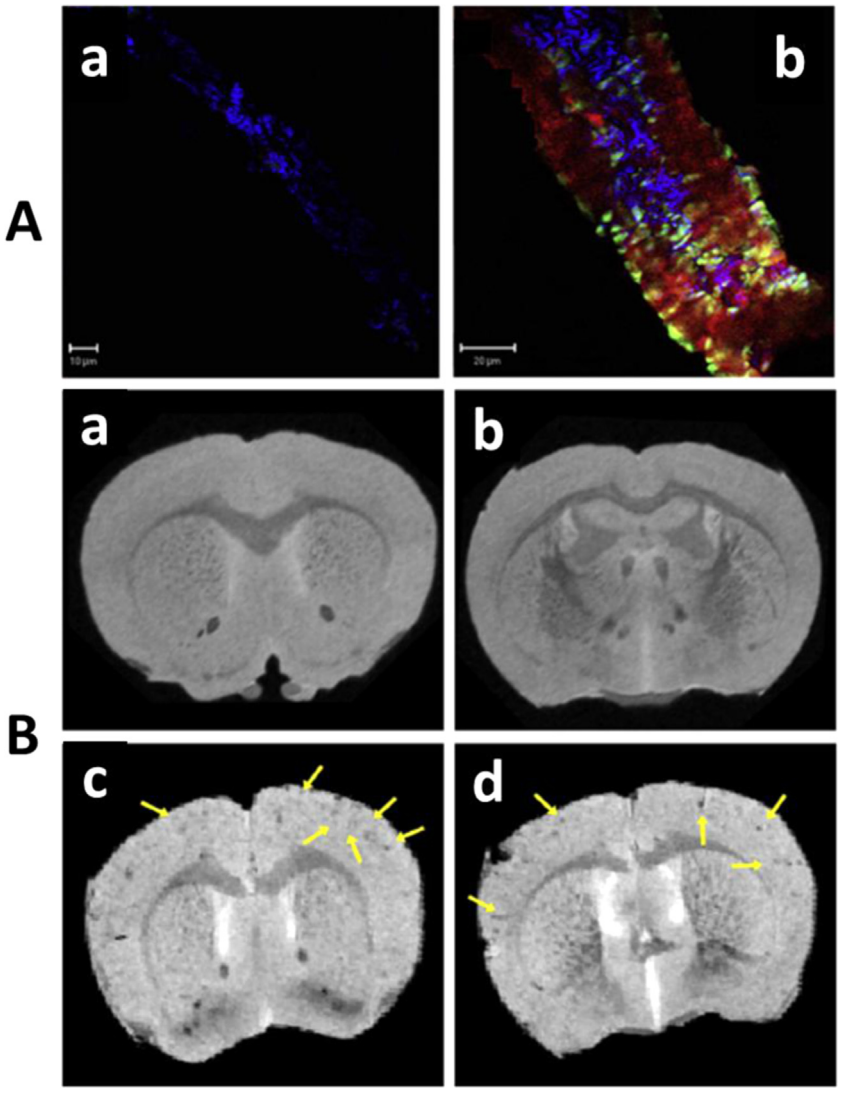

Fig. 6. Presentation of AF647-nanovehicles uptake in brain arteriole of wild type mouse (A) and APP transgenic mouse (B). MRI study of Gd-DTPA-nanovehicles in wild type (WT) mice (C and D), and Gd-DTPAnanovehicles in APP transgenic mice (E and F). (Figure reprinted ref. Jaruszewski, copyright Elsvier-2014) (Jaruszewski et al., 2014).

73 pg/mL in CSF sample (Gagni et al., 2013). Kaminski Schierle et al. reported β-A assemblies act as energy acceptors for fluorescent proteins. Authors developed a protocol to quantify β-A in real sample and living system based on Förster resonance energy transfer (FRET) sensor to monitor the kinetics of β-A aggregation (Kaminski Schierle et al., 2011). In this research work, FRET was observed between aggregation of β-A and emission spectrum of a yellow fluorescent protein variant (YFP). It was observed that FRET mechanism between YFP (donor) and the β-A aggregate (acceptor) quantified via measuring YFP excited state lifetime using time correlated single photon counting (TCSPC) fluorescence lifetime microscopy. The AS-YFP dominantly aggregated into fibrillary species of neuronal than non-neuronal environments. During this process, the generated toxicity is a function of lifetime signature of intermediate, prefibrillar species in a living organism. Authors presented FRET as a non-invasive tool to characterize species associated with neurodegenerative disorders (Kaminski Schierle et al., 2011).

A sensitive nanoparticle based optical bio-barcode assay was developed for estimating amyloid derived diffusible ligands (ADDL) level in CSF to understand AD pathogenesis (Fig. 7B) (Georganopoulou et al., 2005). A sandwich nanostructured platform was prepared using oligonucleotides modified Au and magnetic nanoparticles bound with ADDL specific antibodies. This developed nano-enable optical bar code method which was sensitive and selective to detect ADDL (<1 pM) in 30 patients. Authors reported that bar-code exhibited high throughput, better than imaging technology, and capable to detect other marker needed for AD monitoring with potential to use at clinical level (Georganopoulou et al., 2005).

An antibody conjugated nano-platform consists of a magnetic core-plasmonic shell nanoparticle attached with hybrid graphene oxide and was developed for label free surface enhanced raman spectroscopy (SERS) based selective separation of β-A from CSF to monitor AD (Demeritte et al., 2015) (Fig. 8). Nanoparticles enabled SSRS fingerprint exhibited high sensitivity due to strong plasmonic coupling and identified β-A and tau protein at 100 fg/mL via magnetic separation. This sensor showed β-A and tau protein detection at 0.312 ng/mL and 0.15 ng/mL, respectively, which is better than ELISA (Demeritte et al., 2015). A localized surface plasmon resonance (LSPR) nano-enabling biosensor was developed by Haes et al. to detect ADDL using specific anti-ADDL antibodies (Haes et al., 2005). A nano-platform of Ag nanoparticles fabricated onto mica substrate using nanosphere lithography (NSL)

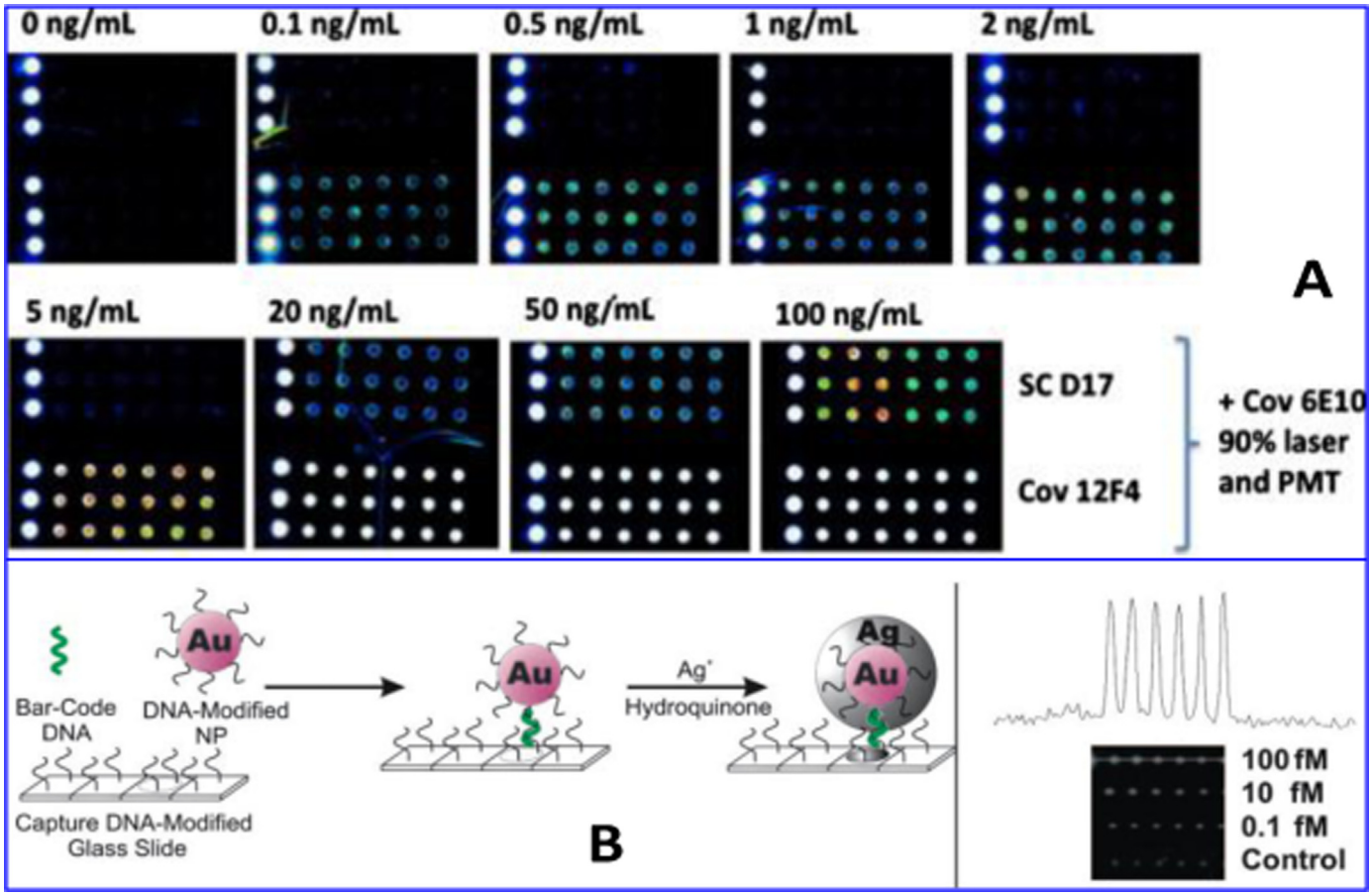

Fig. 7. Illustration of fluorescence imaging at 90% laser power and PMT of $A\beta_{42}$ detection (0–100 ng/mL) using SC-D17 (top arrays) or Cov-12F4 (bottom arrays). (Figure reprinted ref Paola Gagni, copyright Elsvier-2013) (Gagni et al., 2013). Schematic illustration for the fabrication of optical DNA barcode microarrays for the detection of ADDL. An optically active microarray modifies with oligonucleotides captured DNA barcode sequence. NPs modified microarrays to enhance the signal and with oligonucleotides these arrays capture barcode DNA those hybridized to the captured barcode strands. The obtained signal was enhanced using Ag nanoparticles. The signal NPs modified sensing microarray was measured as a function of ADDL level as shown in inset. (Figure reprinted Ref. Georganopoulou, Copyright Science-2015) (Georganopoulou et al., 2005).

was functionalized using self-assembled monolayer (SAM) to prepare a sandwich assay to quantify binding among antigen and secondary antibody to estimate ADDL level. A sensor was developed using this sandwich platform via immobilizing anti-ADDL antibody (100 mM) covalently to detect various concentrations of ADDL (incubation time 30 min) via measuring LSPR shift response. Authors presented LSPR nanosensor as an analytical tool to study oligomerization of low concentrations of β-A precursors (Haes et al., 2005). The β-A aggregation is facilitated by an isoform i.e., apolipoprotein E4 (ApoE4) which is also a dominant risk factor for AD progression. An AuNP based biosensor was developed to detect ApoE4 mediated β-A deposition under biological conditions using LPSR (Kang et al., 2015). ApoE4 binds with only β-A_{1-42} and its specific self-assembled binding onto AuNPs surface due to charge differences was monitored using LSPR shift variation. This sensor showed a detection limit of 1.5 pM with respect to β-A_{1-42} which caused a shift of ~2.9 nm LSPR peak. This real time sensing method exhibited a detection limit of 1.5 pM, selective to only β-A_{1-42} and could be used to explore interaction of ApoE4-Aβ complexes to optimize therapeutic targeting with label-free manner (Kang et al., 2015).

An alkylthiolates-SAM based SPR biosensing method was prepared for label-free detection of 17 β-hydroxysteroid dehydrogenase type 10 (17-HSD10) (Hegnerová et al., 2009). The 17-HSD10 is a multifunctional mitochondrial enzyme associated with AD and investigated as a target marker for the diagnostics of AD. Monoclonal/polyclonal β-A antibody against 17-HSD10 peptide

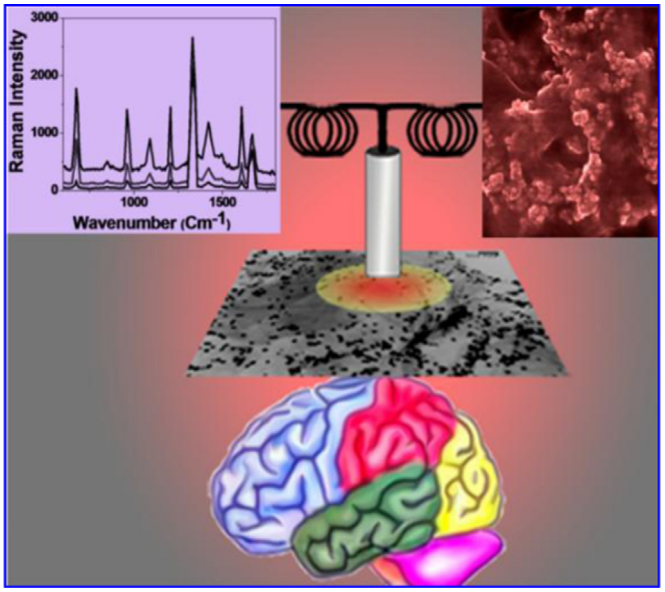

Fig. 8. Illustration of a protocol showing a pathway to develop core-shell nanoparticle/hybrid graphene oxide based multi-functional platform label-free SERS detection of β-A to monitor AD. (Figure reprinted Ref. Teresa Demeritt-2015, Copyright ACS-2015).

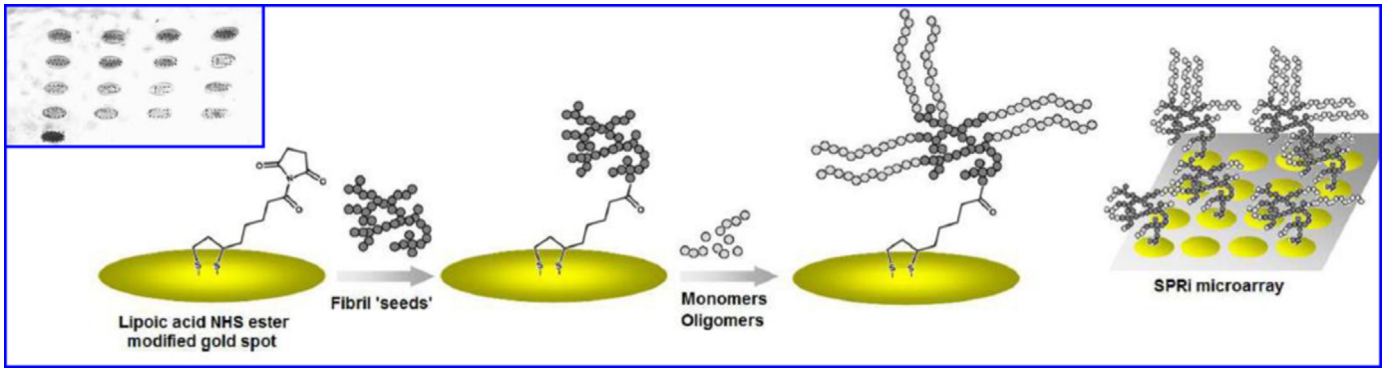

Fig. 9. Representation of SPRi experimental process flow for the detection of β-A fibril elongation using a SPR active Au arrays SPRi. The capturing of β-A elongation on various Au microarrays in shown in inset. (Figure reprinted Ref. Xin R. Cheng, Copyright ACS-2013) (Cheng et al., 2013).

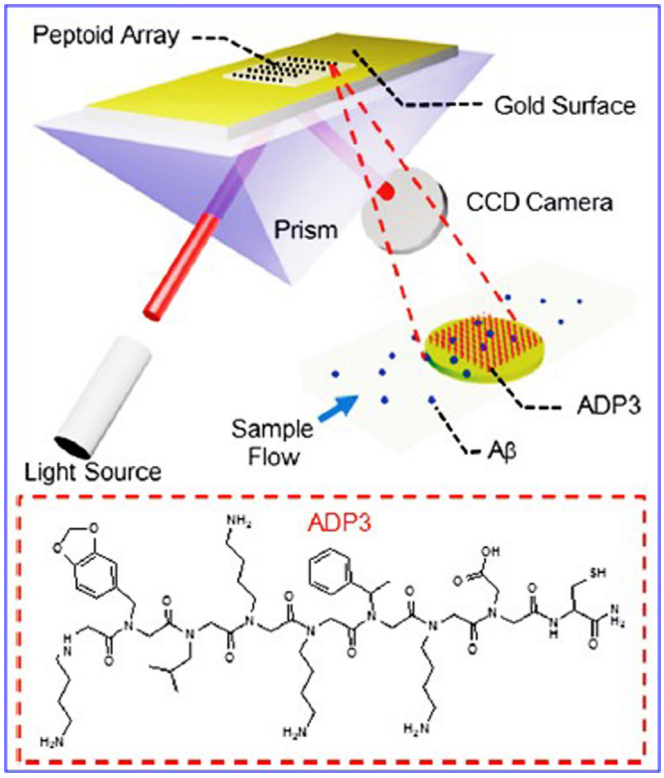

Fig. 10. Demonstration of ADP3 peptoid modified Au array based SPRi for detecting antibodies against β-A 42 in human serum. On serum injection in a flow cell the β-A was captured by ADP3 led to change in refractive index of array. This signal change was detected using a CCD camera. (Figure reprinted Ref. Zijian Zhao-2015, copyright RSC-2015) (Zhao et al., 2015).

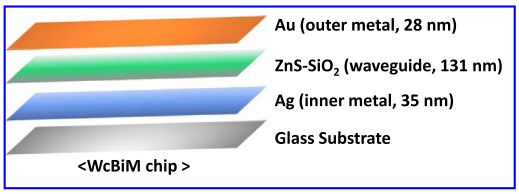

Fig. 11. Illustration of waveguide-coupled bimetallic (WcBiM)-SPR. (Figure reprinted Ref. Yaon Kyung Lee-2014, Copyright PLoS One-2014) (Lee et al., 2014).

was immobilized onto SAM platform via amino coupling chemistry to detect synthetic peptide of 14 amino acids from the 17-HSD10 molecule (residues 133–146) and whole enzyme 17-HSD10. Author also detected 17-HSD10 enzyme in artificial CBF at ng/ml levels (Hegnerová et al., 2009). Cheng at al reported that many human protein misfolding disorders in AD are related with β-sheet-rich amyloid fibrils accumulation (Cheng et al., 2013). The β-A peptides showed interaction with metals such as Zn^{2+}, Cu^{2+}, and Fe^{3+}, resulting in reactive oxygen species (ROS) production. This interaction process based on nucleation-dependent β-A aggregation or seeding propagate fibril formation, was detected using SPR imaging. To perform SPRi, a single chip was fabricated for simultaneous monitoring of the effects of multiple modulators on fibril elongation (Fig. 9). Authors demonstrated that fibril seeds formed via incubation of β-A in metals promoted monomer elongation in comparison of β-A alone or in the presence of metal-chelating polyphenol, (-)-epigallocatechin-3-gallate (EGCG). The results obtained using SPRi were validated using TEM and thioflavin T (ThT) and confirmed that varying degree of β-A aggregation associated with different elongation rates in the SPRi experiment. These results can be explored to understand several mechanisms to study the effect of small molecules on aggregation pathway in neurodegenerative diseases (Cheng et al., 2013).

Zhao et al. used SPRi for detecting β-A through ADP3 peptoid -a synthetic N-substituted oligoglycine and an antigen surrogate to identify and isolate target antibodies in body fluids (Zhao et al., 2015). Authors fabricated an Au coated glass chip to perform SPRi as a function of ADP3 concentration (48–30 mM) collected from AD patients. The capturing of ADP3 onto chip was confirmed using antibodies against $\beta\text{-A}_{1-42}$ and human IgG (Fig. 10). The observed signal related with anti-β-A found higher than obtained from anti-IgG confirmed selectivity of ADP3 to $\beta\text{-A}_{1-42}$ in human serum. On the basis of these findings, authors reported that AD patients possess a specific defect that lower down the level of IgG and upregulate β-A 42 in the serum (Zhao et al., 2015).

Lee et al. fabricated a waveguide-coupled bimetallic (WcBiM)-SPR chip of SAM for the detection of β-A levels (Lee et al., 2014) (Fig. 11). This modified SPR system exhibited better performance than Au based system due to narrow full-width-at-half-maximum (FWHM). Anti- β-A antibody was immobilized onto WcBiM-SPR chip detecting β-A level ranging from 100–2000 pg/mL. The WcBiM-SPR was found to be selective and detect β-A level at 500 pg/mL. Authors claimed that optimized WcBiM and SPR chip with suitable surface modification according to intensity interrogation detection protocol can be used in place of other biomarkers (Lee et al., 2014).

Neuroimaging methodologies namely MRI, PET, SPET, NIR, SPR, and SPRi, briefly explained above, are capable to detect β-A in biofluids to monitor AD progression and pathogenesis. However, these methods are limited to clinics due to requirement of sophisticated equipments and high expertize to operate. To overcome these shortcomings, electrochemical sensing methodologies are being investigated for rapid, selective and sensitive detection

of β-A in bio-fluids for AD monitoring. Recent advancement in electrochemical β-A sensing technology-based on nano-enabling sensing material, utilization of various transduction methods, and automated sensing strategies to detect β-A at pM are discussed in next section.

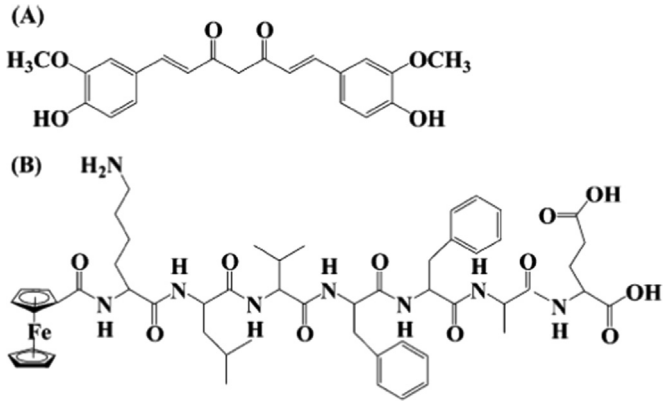

Fig. 12. Chemical structure of curcumin (A) and Fc-KLVFFAE (B) (Figure reprinted Ref. Veloso, copyright Elsevier-2012) (Veloso and Kerman, 2012).

4. Advancements of electrochemical β-A bio-sensing

Rapid, sensitive, and selective detection of β-A for AD management is crucial. Although, available techniques have shown potential to detect β-A at clinical level but their implementation to detect β-A is not in practice. Due to the salient features such as fast, selective and sensitive detection, electrochemical immune-sensing methodology has been adopted rapidly for target marker detection at pg/mL level (Kaushik et al., 2014). The introduction of nano/micro electrodes, nanostructured sensing materials, micro-electronics, and miniaturized sensing transducers in electrochemical sensor fabrication have shown to improve the device performance (Cruz et al., 2014; Kaushik et al., 2015). The integration of a miniaturized highly sensitive sensors with the microfluidic system and miniaturized potentiostat (M-P) has been reported to monitor biomarkers with reduced form factors (Cruz et al., 2014; Kaushik et al., 2015). Further, efforts are being made for developing these sensing systems at POC levels for personalized health monitoring. For example, our recently developed M-P was capable of performing electrochemical immuno-sensing to detect cortisol, a potential psychological stress biomarker, at pM level within 40 min and validated with classical ELISA method. The test results were found similar in both detection methods in specimens obtained from farm workers and HIV patients (Cruz et al., 2014; Kaushik et al., 2015). Similar approach can be used for

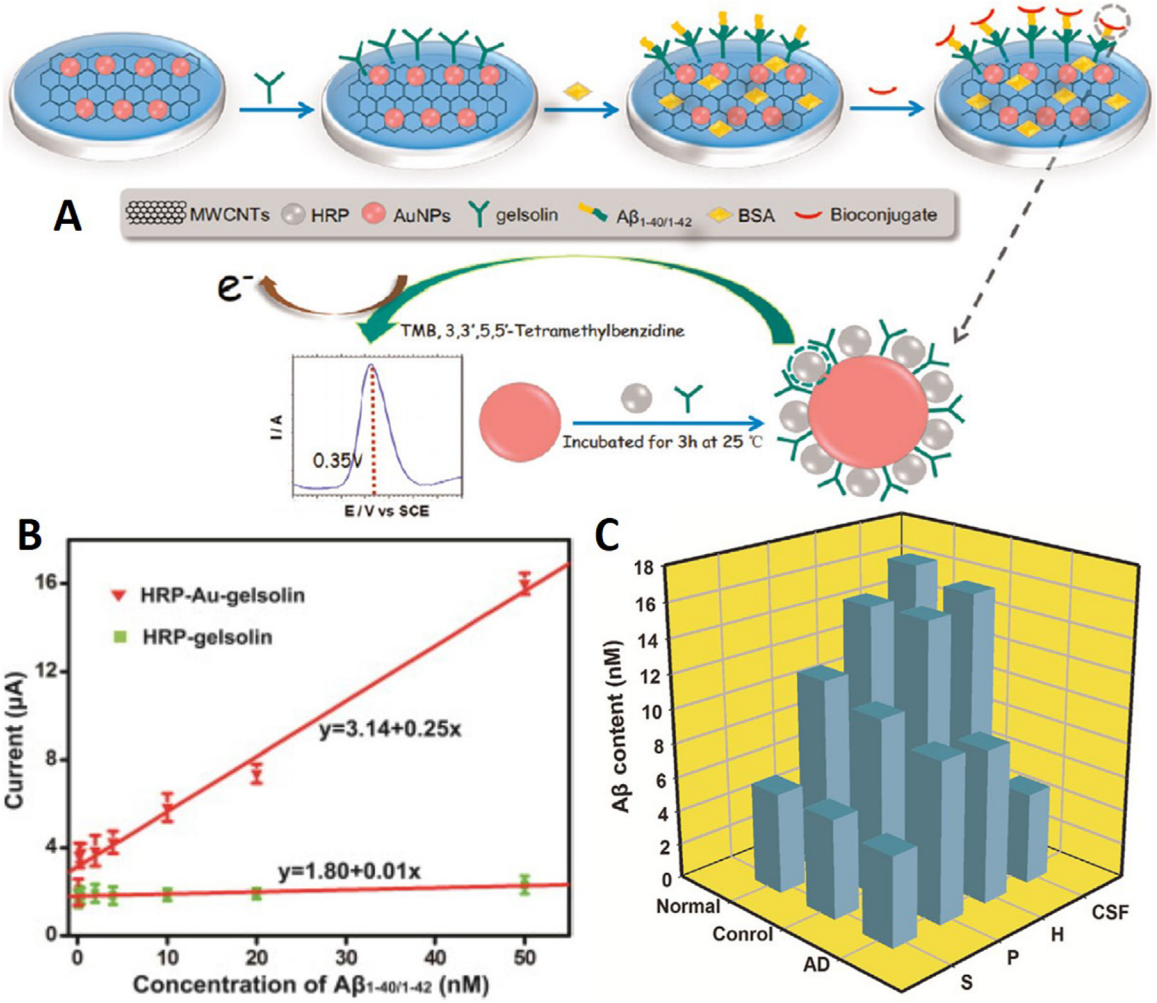

Fig. 13. (A) Fabrication of gelsolin-bound electrochemical β-A biosensor, (B) a linear calibration curve plotted as DPV response and β-$A_{1-40/1-42}$ concentrations (0.1, 0.2, 0.4, 2, 4, 10, 20, 50 nM). The developed HRP–Au–gelsolin and HRP–gelsolin was used a as an electroactive, and (C) presentation of β-A variation in CSF. (Figure reprinted Ref. Yan Yan Yu-2015, copyright Elsevier-2015) (Yu et al., 2015).

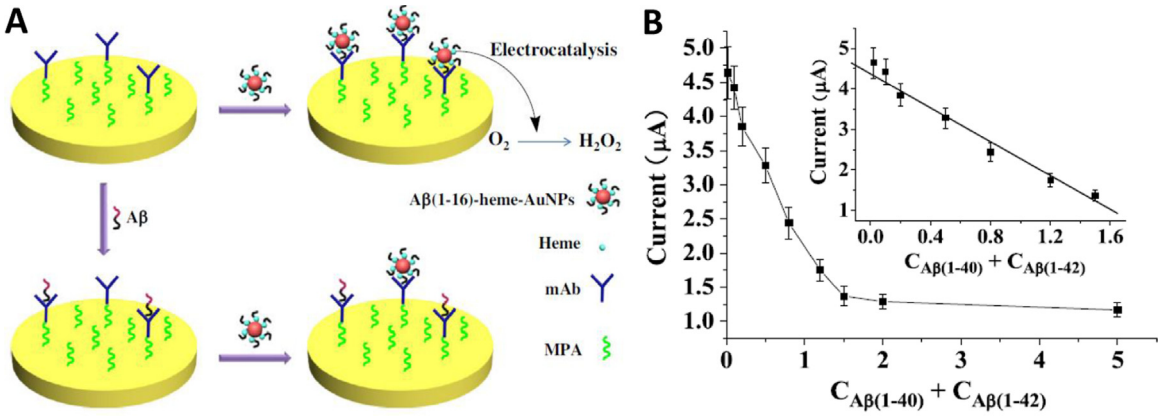

Fig. 14. Illustration of electrochemical biosensor based on β-A_{1-16}-heme-AuNPs to detect β-A based on specific mAb. (B) A calibration curve plotted between electrochemical response and β-A concentrations (0.02–5.00 nM). A linear calibration curve was obtained using 0.02, 0.10, 0.20, 0.50, 0.80, 1.20 and 1.50 nM β-A level. (Figure reprinted Ref. Lin Liu-2013, copyright Elsevier-2013) (Liu et al., 2013).

the development of a β-A monoclonal antibody based electrochemical immuno-sensor to detect β-A as low as pM levels within ~40 min compared to time consuming ELISA test at nM levels in a fully equipped laboratory setup. The outcomes obtained from such sensing systems can be used for rapid screening and monitoring of AD in patients.

A label free electrochemical biosensor based on screen printed carbon paste (SPCP) electrode and square wave voltammetry (SWV) transduction technique was fabricated by Veloso et al. to detect β-sheet breaker pentapeptide (LPFFD, FibIII), which is an inhibitor of β-A fibrils and oligomers (Fig. 12) (Veloso and Kerman, 2012). Authors performed SWV to monitor interaction of β-A_{1-42} with FibIII at early stage aggregation. SWV signal was measured by monitoring oxidation of its single tyrosine (Y10) residue. The findings were validated using fluorescence imaging using ThT dye as an imaging agent for β-A peptides (Veloso and Kerman, 2012). Electrochemical detection of β-A in combination with HPLC was explored by Zhang et al. via monitoring oxidation of Fc, attached to N-terminus to KLVFFAE, inhibiting the aggregation of β-A_{1-42} (Zhang et al., 2013a). In this work, authors used curcumin as an electroactive component to inhibit β-A aggregation. HPLC-electrochemical enabled separation of soluble Fc-KLVFFAE molecules from curcumin to control aggregation in real time manner (Zhang et al., 2013a).

Electrochemical techniques such as SWV, differential pulse voltammetry (DPV), and cyclic volatammetry (CV) was utilized for rapid and label-free detection of β-A_{1-40} and β-A_{1-42} using glassy carbon electrode (GCE) (Vestergaard et al., 2005). Authors utilized tyrosine (Tyr) as a redox moiety and monitored the oxidation signal to detect β-A peptide level. The β-A aggregation altered structure conformation and led to changes in Tyr oxidation signal. Authors reported DPV based sensing performance better than CV and SWV. This sensor exhibited a detection limit of 0.7 ng/mL with a relative standard deviation of 0.3–1.4% and 0.4–3.0% for β-A_{1-40} (incubation time of 300 min) and β-A_{1-42} (incubation time 750 min), respectively (Vestergaard et al., 2005). Li et al. developed a peptide-based SWV electrochemical biosensor via functionalizing an electrode surface using oligopeptide to detect β-A_{1-42} soluble oligomer (Li et al., 2012). Author reported that the surface electron transfer dynamics of peptide-based biosensor differentiated the presence and absence of β-A. This sensing approach was employed for assaying of β-A_{1-42} soluble oligomer for quantitative estimation. Results of the presented studies showed that developed sensor exhibited a detection limit of 240 pM with fairly detectable signal-on response and a linear range 480 pM to 12 nM. However this sensor need to be optimized using real samples (Li et al., 2012).

Metal [Fe(II), Cu(II) and Zn(II)]-induced β-A aggregation increases ROS production to induce more damage to brain cells (Hung et al., 2012). The SWV based biosensor was developed to understand the kinetics of β-A aggregation in presence and absence of metals using Thr as signal. The results of this study showed that Zn and Fe metal ions increase β-A aggregation. This sensor was responsive for β-A to analyze the effect of metal chelating histidine-rich region i.e., the hydrophobic part of peptide (Hung et al., 2012). These results established a mechanism of β-A aggregation on adding metal-chelating agents.

A sensitive electrochemical nano-probe was fabricated by Yu et al. to detect soluble β-$A_{1-40/1-42}$ peptides using a bio-conjugate of horseradish peroxidase (HRP)-Au nanoparticles (NPs)–gelsolin (Yu et al., 2015). This group explored specific binding between gelsolin and β-A as an alternative way to detect β-A. To develop a sandwich sensor array to detect soluble β-$A_{1-40/1-42}$, a nano-hybrid of HRP-AuNPs–gelsolin was fabricated using one-pot functionalization of AuNPs with HRP and gelsolin. Soluble β-A peptides were captured by gelsolin via specific binding and an electrochemical signals were performed via measuring oxidation/reduction of HRP labeled on AuNPs through signal generated by hydrogen peroxide (H_2O_2) production (Fig. 13). Presented sensor exhibited a detection limit of 28 pM with respect to β-$A_{1-40/1-42}$. Authors claimed that this newly developed sensor may generate information to understand pathological events in AD brain needed for the diagnosis of AD progression (Yu et al., 2015).

A sensitive and selective electrochemical sensing strategy to detect β-A peptides using AuNPs modified with heme β-A_{1-16}, an electroactive agent exhibiting electro-catalytic O_2 reduction has been reported (Liu et al., 2013). Specific monoclonal antibody (mAb) with ability to bind with N-terminus of β-A was immobilized onto AuNPs-heme/β-A_{1-16}. The adsorption of AuNPs-heme/ β-A_{1-16} onto sensing surface is prevented due to the captured β-A by mAb resulting in decreased voltammetric response. This developed sensor showed a β-A detection range from 0.02 to 1.50 nM with a detection limit of 10 pM (Fig. 14). This sensor was suggested to detect β-A in CSF samples containing β-$A_{1-40/1-42/1-16}$ (Liu et al., 2013).

An antibody-free electrochemical sensor was prepared via immobilizing alkaline phospahte-cystein-Prp (95–115) peptide onto Au electrode for selective detection of β-A oligomers using CV technique (Liu et al., 2015). An outer-sphere to inner-sphere mechanism based electrochemical redox cycling of ferrocene was used to amplified signal to achieve improved sensitivity. This sensor exhibited a detection limit of 3 pM. This sensor showed better results than conventional sandwich-like detection procedure. Authors proposed that sensor based on surface

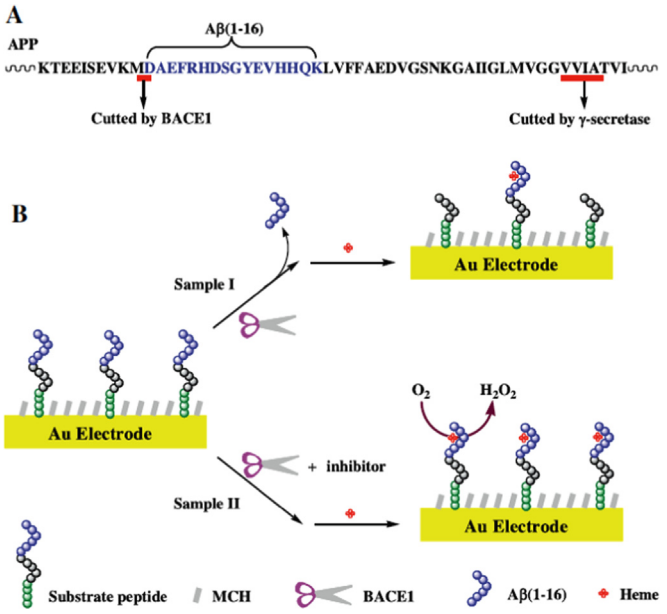

Fig. 15. (A) APP sequence containing β-A segment and illustration of electrochemical sensor to probe BACE1 activity and screening. (Figure reprinted Ref. Ning Xia, Copyright Elsevier-2015) (Xia et al., 2015).

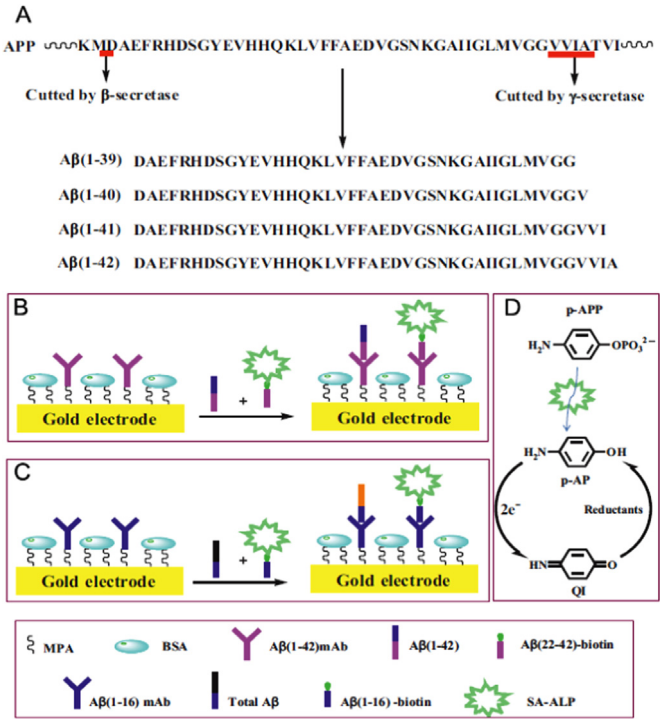

Fig. 16. β-A native sequence isolated from and demonstration of β-A_{1-42}, and total β-A detection. (Figure reprinted Ref. Liu, BIOS 2014, Copyright Elsevier-2014) (Liu et al., 2014).

functionalization using nanomaterials and other electro-active enzymes could amplify signal to achieve enhanced β-A oligomer sensing performance. This method was selective and potential to be used for clinical diagnosis of AD (Liu et al., 2015). The CV based label and enzyme free biosensor was developed for the monitoring of β-site amyloid precursor protein cleaving enzyme 1 (BACE1), an aspartic protease that promotes β-A peptide production (Xia et al., 2015). This sensor (Fig. 15) was also tested for the inhibitor of BACE1. During sensing, a peptide–heme complex was formed on sensing surface that showed electro-catalytic reduction of O_2 molecule. The suppression of BACE1 due to effect of inhibitor i.e., IC-50 yielded a higher electrochemical signal. This sensor was responsive at 15.5 nM level of IC-50. This reported method was simple and low cost assay but the detection limit was comparatively high (Xia et al., 2015).

AuNPs decorated SPCE based disposable electrochemical immunosensor was developed to detect β-A_{1-42} using a competitive immunoassay protocol (Rama et al., 2014). A competitive immunoassay was fabricated by immobilizing biotin-β-A_{1-42} on electrode surface, wherein β-A compete against anti- β-A_{1-42} antibody. CV based electrochemical sensing was performed using an alkaline phosphatase labeled anti-rabbit IgG antibody, which generated an analytical signal via enzymatically generated silver. This sensor exhibited a detection limit of 0.1 ng/mL and a detection range varied from 0.5 to 500 ng/mL ($n=3$) which is within the physiological range. Authors claimed that such fabricated immunosensor is very simple and can be integrated in a sensing device to developed portable sensing system (Rama et al., 2014). A sensitive and selective electrochemical biosensor was developed to detect β-A_{1-42} and total β-A in sample via immobilizing anti-β-A antibody onto Au electrode (Liu et al., 2014). A competitive immunoassay (Fig. 16) was fabricated using a streptavidin-conjugated alkaline phosphatase (SA-ALP) and biotinylated β-A peptides to capture antibody-modified electrodes. For biosensing, an electrochemical signal of p-AP redox cycle generated by tris(2-

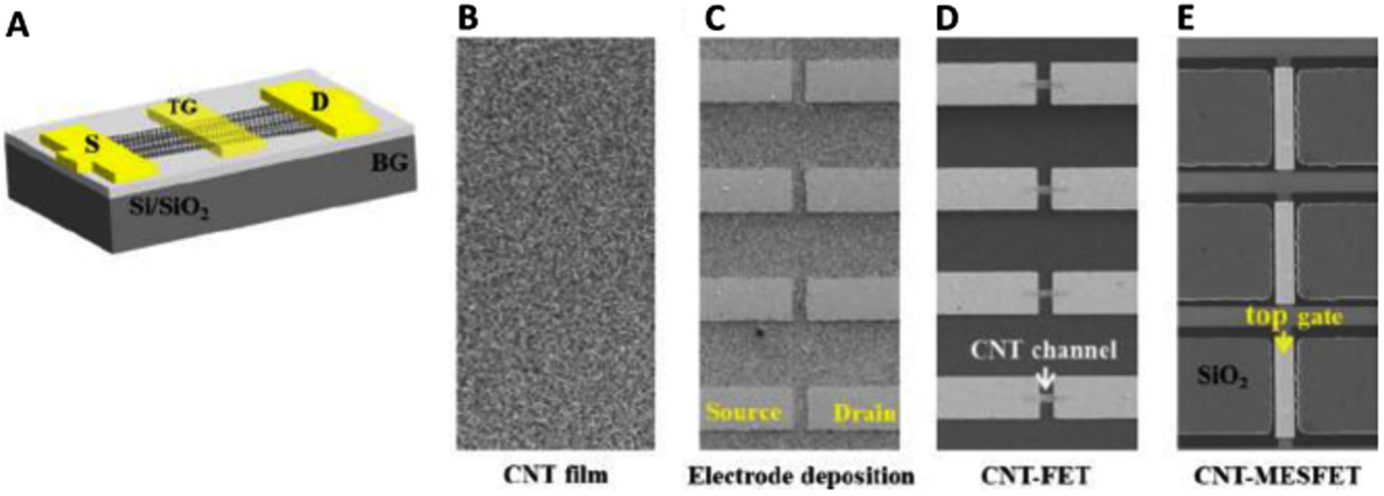

Fig. 17. Illustration of CNT-MESFET device fabrication. (Figure reprinted Ref Oh-2013, copyright Elsevier-2013) (Oh et al., 2013).

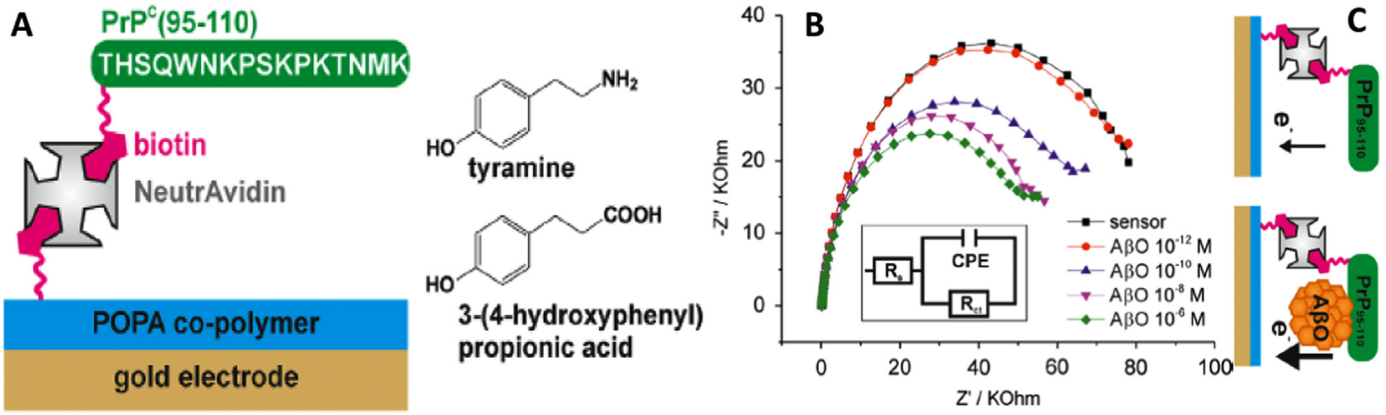

Fig. 18. An LBL based EIS sensor fabricated onto Au coated POPA (polytyramine/poly 3-(4-hydroxyphenyl propionic acid)) using electro-polymerization. The sensing surface was modified by tyramine moieties using NHS-biotin chemistry. This surface was further modified with NeutrAvidin to bind with biotinylated PrPC (95–110). This EIS Biosensor detected β-A oligomers (pM to μM total Aβ peptide concentration) using incubation time of 20 min and PBS electrolyte containing 10 mM Fe (II)/Fe(III) redox probe. (Figure reprinted Ref. Rushworth, Copyright Elsevier-2014) (Rushworth et al., 2014).

carboxyethyl)phosphine (TCEP) was monitored as a function of β-A concentration. A reduction of electrochemical signal was obtained on increasing β-A level which compete against β-A anchoring antibody. This sensor exhibited a detection limit of 5 pM with respect to β-A_{1-42} and total β-A selectively in CSF samples which also contained β-$A_{1-40/1-42/1-16}$, proving its potential for early diagnosis (Liu et al., 2014).

A carbon nanotube (CNT) film based biosensor consists of a metal semiconductor field effect transistor structure (MESFET, Fig. 17), where Au serves as a gate material, developed for β-A detection (Oh et al., 2013). Authors used HRP as a model element for electrochemical signal generation. The anti-HRP antibodies were immobilized onto Au with protein G or auto displayed Z-domains of protein-A. The CNT-MESFET biosensor was sensitive than CNT-FET based biosensors due to high loading of antibody in a desired orientation. This lead to low detection limits of 1 pg/mL in human serum. This sensor showed β-A sensing from 1 pM to 1 ng/mL in real time manner in blood samples FET (Oh et al., 2013).

Along with above mentioned voltammetry techniques, the electrochemical impedance spectroscopy (EIS) has also been explored to detect β-A for the assessment of AD. The EIS method is one of the best non-invasive analytical tool and is being explored for monitoring biological phenomena such as protein-protein interaction (Bogomolova et al., 2009; Chang and Park, 2010; Franks et al., 2005), bio-sensing (Kaushik et al., 2010), nano-toxicity (Shah et al., 2014) and tumour drug interaction (Luongo et al., 2013). An EIS based detection method, using 10 mM $[Fe(CN)_6]^{3-/4-}$ as the redox probe in 50 mM PBS with 100 mM NaCl (pH 7.4) at a potential of 0.30 V was developed to detect β-A. This system exhibited β-A sensing via interaction of a polyphenolic compound i.e. resveratrol with β-A (Hung et al., 2013). The β-A aggregation and its inhibition using resveratrol was studied by monitoring variation in charge transfer resistance (Rct). The results of this study was validated using ThT fluorescence assay and TEM imaging, confirming that EIS is able to analyze β-A_{1-40} aggregation in-vitro (Hung et al., 2013).

A label-free EIS biosensor (Fig. 18) was developed using biotinylated cellular prion protein (PrPc-residues 95–110) for the specific detection of β-A oligomers (Rushworth et al., 2014). PrpPc (95–110) is a synaptic protein and mediated neuronal binding and β-A oligomer toxicity. This protein was used to fabricate β-A impedimetric biosensor using layer-by-layer approach based biotin/neutravidin bridge to polymer-functionalized Au-SPE. This sensor exhibited a linear β-A sensing phenomena with a detection limit of ~0.5 pM. However this highly sensitive sensor needs many

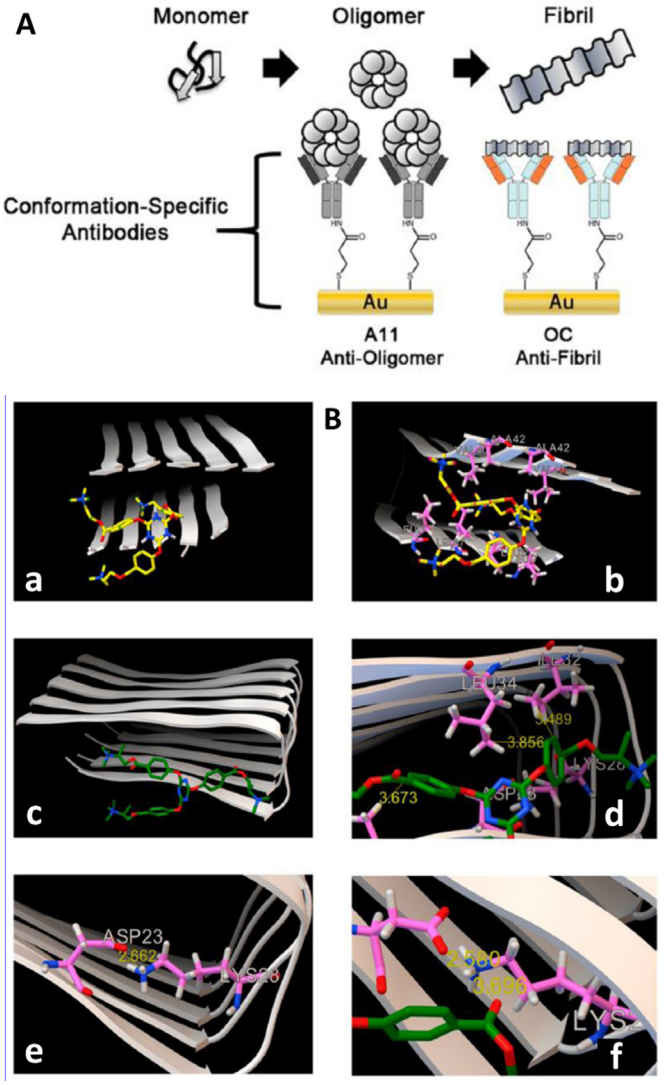

Fig. 19. Illustration of a detection principle to monitoring β-A1–42 fibrils and toxic oligomers based on conformational specific antibodies loading using EIS, (B) Demonstration of molecular modeling simulations to confirm the binding affinities of TAE-1 (a, b) and TAE-2 (c, d) to Aβ1–42 fibrils (2BEG)57 using Autodock Vina run at an exhaustiveness of 400. Results confirmed that TAE-1 and TAE-2 showed maximum binding affinity (evaluated based on estimating binding energy (ΔGb, kcal/mol)). (Figure reprinted Ref. Veloso, Copyright ACS-2014) (Veloso et al., 2014).

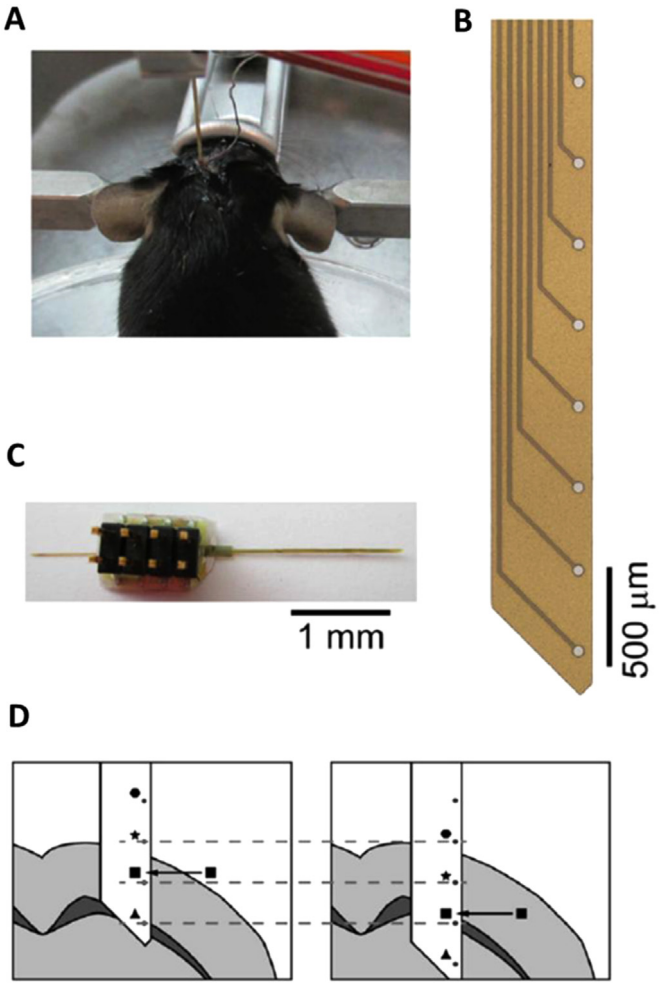

Fig. 20. An illustration of a post mortem stereotaxically implanted mouse (a), detection probe (b), polyimide probe to measure an array of eight 50 μm diameter platinum electrodes, and representation of the probe insertion into the brain and impedance spectra were recorded at every 100 μm step. (Figure reprinted Ref. Beduer, Copyright IOP-2015) (Beduer et al., 2015).

optimizations related reproducibility and stability in order to develop sensor for clinical practices (Rushworth et al., 2014).

An EIS sensor, (Fig. 19) fabricated via functionalizing Au disc with SAM of 3,3′-dithiobis (sulfosuccinimidyl) propionate (DTSSP) to immobilize specific antibodies (OC and A11) for rapid aggregation processes of oligomeric and fibrillary states of β-A_{1-42} (Veloso et al., 2014). The variation in Rct value of redox moieties Fe (II)/Fe(III) was analyzed to monitor interaction between antibody and various concentration of β-A. This developed platform was used to check the performance of sym-triazine-derived aggregation modulators (TAE-1 and TAE-2) to inhibit β-A aggregation. To validate sensing performance, the β-A oligomer/fibrillar formation was also evaluated using ThT fluorescence, MALDI-MS MALDI, and western blot. Results of this study suggested that TAE-1 binds with terminal hydrophobic residues of the $Aβ_{1-42}$ fibril (−6.2 kcal/mol) and TAE-2 binds with central hydrophobic region (−6.7 kcal/mol). This sensor is found good for β-A screening and monitoring Aβ-targeted drug therapies AD (Veloso et al., 2014).

A sensitive EIS sensor was fabricated via immobilizing specific β-A antibody onto AuNPs sputtered onto anodic aluminum oxide (AAO) nano-hemisphere array to detect β-A_{1-42} (Wu et al., 2014). AuNPs deposited onto microarrays increased surface area led to higher loading of IgG using EDC-NHC chemistry. The specificity of β-A_{1-42} and antibody were studied using western blot. EIS response study was performed as a function of charge transfer resistance and β-A concentrations. This sensor exhibited a detection limit of 1 pg/mL, detection range of 1 pg/mL to 10 ng/mL and followed a linear equation as Rct=29098*log [β-A_{1-42}]+90150 with a regression coefficient of 0.9916. The aggregation (1500–2000 nm) of β-A on sensing surface was measured using SEM and AFM. This sensor required 25 μL of sample volume and 3 minutes to perform β-A sensing. The results of this study were validated using ELISA and western blot (Wu et al., 2014).

A label free EIS β-A biosensor based on carbon disposable electrochemical printed (CDEP) chip was fabricated by Lien et al. for the detection of β-A levels (Lien et al., 2015). This group optimized surface chemistries to fabricate SAM-AuNPS based β-A biosensor to achieve higher sensitivity. The sensor surface was modified using protein-G to achieve optimum orientation of anti-β-A antibody. Biosensor fabricated using SAM-AuNPs showed three orders high sensitivity, detection limit of 0.57 nM and a detection range 2.65 nM to 2.04 μM. This sensor was disposable, cheap, and was able to detect low level of β-A (Lien et al., 2015).

A microfluidic based EIS biosensor (Fig. 20) was fabricated using pretreated magnetic beads as sensing materials to detect β-A (Shin et al., 2015). Pretreated magnetic beads were injected in fluidic micro channel and positioned on microarrays. Further, the Rct values were measured on adding β-A concentrations aggregated on magnetic beads in a fluidic channel. This reported EIS sensing device detected β-A at pg/mL without using biomolecule (Shin et al., 2015). Beduer et al., explored electrical impedimetirc measurement for the post-mortem in APPPS1 transgenic mice

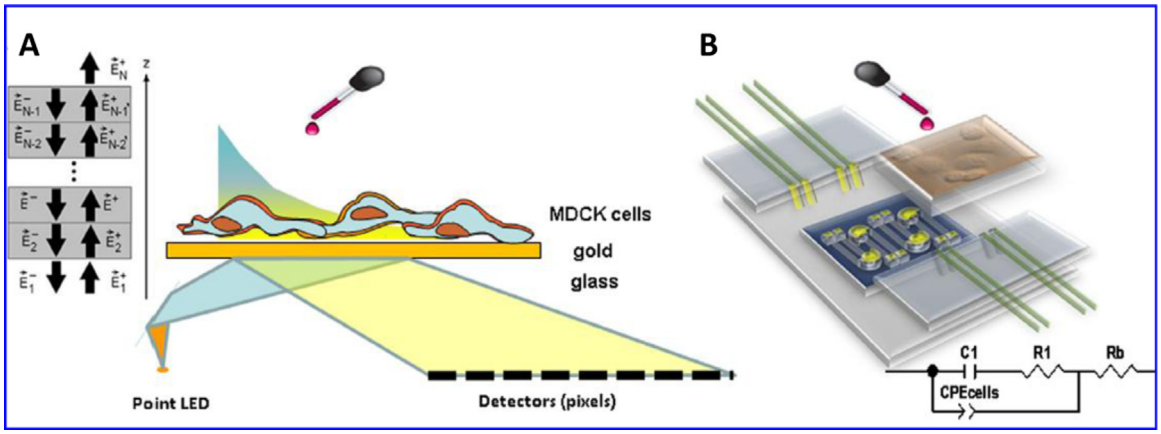

Fig. 21. (A) Illustration of an experimental set-up containing SPR and EIS to detect β-A in living cells. (Figure reprinted Ref. Gheorghiu, Copyright Elsevier-2014) (Gheorghiu et al., 2014).

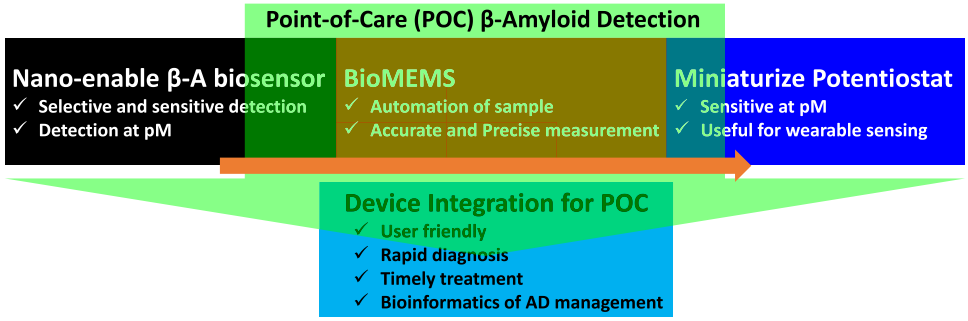

Fig. 22. A vision for β-A detection at POC of AD monitoring and diseases management.

brains to study amyloidogenesis for monitoring pathological hallmark of AD (Beduer et al., 2015). A flexible probe [Fig. 20] with embedded micrometric electrodes array was designed to detect senile plaques composed of β-A peptides via localized impedance measurements. Thus developed method was capable to focus on deep brain of APPPS1 mice and showed impedance signal variation with the percentage of β-A plaque load. This method was also able to monitor aging affect in AD APPPS1 mice model. This model can be useful to improve the diagnosis and monitoring of β-A loads *in-vivo* after optimizing operational parameters. The integration of this probe inside AD brain provided continuous monitoring of Aβ plaque progression and also for β-A-targeting therapeutic strategies evaluation (Beduer et al., 2015).

Recently, a multi-parametric label-free analysis system based on SPR and EIS (Fig. 21) was investigated to monitor the progression of epithelial cell culture of Madin Darbey Canine Kidney (MDCK) exposed with β-A_{1-42} peptides (Gheorghiu et al., 2014). Synergistically, SPR and EIS based approaches were capable to monitor biphasic cellular response generated via adding nonlethal dose of β-A onto sensing surface that caused changes in cell substrate adherence and cell to cell tight junction or cytoskeletal remodeling. The obtained change in electrical response was validated using western blot and AFM microscopy. This method was explored to connect β-A_{1-42} fibrils with the modified expression of barrier proteins i.e., occludin and claudin in real time manner. The EIS and SPR were able to explore the dynamic effect of β-A fibrils on cell layers that provides general information to achieve a label free cellular sensing (Gheorghiu et al., 2014).

5. Towards β-A detection at point-of-care application

Few electrochemical systems, (Rushworth et al., 2014; Veloso et al., 2014), ELISA assays (Schenk et al. 1999; Yang et al. 2003), optical immunoassays, and SPR (Haes et al., 2004; Hegnerová et al., 2009) based approaches have been investigated for β-A detection in real samples. As of now, it is difficult to use the state-of-the art facility and expertize at POC application due to need of high expertize and sophisticated laboratory set-up. Thus developing a β-A biosensing system at POC application has significance for personalized health care of individuals. Recently, M-P based electrochemical immune-sensors were developed for biomarker detection with desired performance (Cruz et al., 2014; Kaushik et al., 2015; Pasha et al., 2014). Besides this, significant success has been made to design and develop BioMEMS for automated biosensing at pM level. Therefore, we hypothesized that, at POC, β-A can be detected at pM level on successful integration of nano-enabled component required to make sensing systems. Such devices can be used for rapid screening and monitoring of AD in patients and can facilitate the disease management for therapeutics decision. The β-A sensing in desired bio-fluids at POC will provide useful bioinformatics useful for clinicians to monitor AD progression to decide treatment for patients with neurodegenerative disorder (Fig. 22). Such devices could be potential analytical tool for AD management to optimize therapeutics.

6. Conclusions

This review summarizes recent advancements in nanostructured sensing platforms and transduction techniques to develop an effective electrochemical biosensor to detect β-A in bio-fluids. Although, available sensors are limited at clinical level but on successful integration of nano enabled device components, miniaturized systems can become capable of β-A detection at POC application. This review is a call to scientists for exploring multi-

disciplinary research to fabricate nano-enabled miniaturized electrochemical β-A biosensor towards β-A detection for diagnosis and monitoring of AD diseases. Such developed sensing systems would be useful to generate bioinformatics needed for the management of AD for patients those affected by AD alone and along with other neurological disorders. These nanosensors have bright future prospects to detect and manage AD at POC for therapeutic purposes.

Acknowledgments

Authors acknowledge NIH grants namely RO1-DA027049, R21-MH 101025, RO1-DA 034547, R01-DA037838, and 1R01-DA-040537-01.

References

Adle-Biassette, H., Levy, Y., Colornbel, M., Poron, F., Natchev, S., Keohane, C., Gray, F., 1995. Neuropathol. Appl. Neurobiol. 21 (3), 218–227.
András, I.E., Toborek, M., 2013. IUBMB Life 65 (1), 43–49.
Beduer, A., Joris, P., Mosser, S., Fraering, P.C., Renaud, P., 2015. J. Neural Eng. 12 (2), 024001.
Bogomolova, A., Komarova, E., Reber, K., Gerasimov, T., Yavuz, O., Bhatt, S., Aldissi, M., 2009. Anal. Chem. 81 (10), 3944–3949.
Butterfield, D.A., Drake, J., Pocernich, C., Castegna, A., 2001. Trends Mol. Med. 7 (12), 548–554.
Chang, B.-Y., Park, S.-M., 2010. Annu. Rev. Anal. Chem. 3, 207–229.
Cheng, X.R., Hau, B.Y., Veloso, A.J., Martic, S., Kraatz, H.B., Kerman, K., 2013. Anal. Chem. 85 (4), 2049–2055.
Claeysen, S., Bockaert, Jl, Giannoni, P., 2015. ACS Chem. Neurosci. 6 (7), 940–943.
Cruz, A.F.D., Norena, N., Kaushik, A., Bhansali, S., 2014. Biosens. Bioelectron. 62, 249–254.
Csernansky, J., Wang, L., Swank, J., Miller, J., Gado, M., McKeel, D., Miller, M., Morris, J., 2005. Neuroimage 25 (3), 783–792.
Demeritte, T., Viraka Nellore, B.P., Kanchanapally, R., Sinha, S.S., Pramanik, A., Chavva, S.R., Ray, P.C., 2015. ACS Appl. Mater. Interfaces 7 (24), 13693–13700.
Fonseca-Santos, B., Chorilli, M., Palmira Daflon Gremião, M., 2015. Int. J. Nanomed., 4981.
Franks, W., Schenker, I., Schmutz, P., Hierlemann, A., 2005. IEEE Trans. 52 (7), 1295–1302.
Fu, H., Cui, M., Zhao, L., Tu, P., Zhou, K., Dai, J., Liu, B., 2015. J. Med. Chem. 58 (17), 6972–6983.
Gagni, P., Sola, L., Cretich, M., Chiari, M., 2013. Biosens. Bioelectron. 47, 490–495.
Georganopoulou, D.G., Chang, L., Nam, J.-M., Thaxton, C.S., Mufson, E.J., Klein, W.L., Mirkin, C.A., 2005. Proc. Natl. Acad. Sci. USA 102 (7), 2273–2276.
Gheorghiu, M., David, S., Polonschii, C., Olaru, A., Gaspar, S., Bajenaru, O., Popescu, B. O., Gheorghiu, E., 2014. Biosens. Bioelectron. 52, 89–97.
Green, D.A., Masliah, E., Vinters, H.V., Beizai, P., Moore, D.J., Achim, C.L., 2005. Aids 19 (4), 407–411.
Haass, C., Selkoe, D.J., 2007. Nat. Rev. Mol. Cell Biol. 8 (2), 101–112.
Haes, A.J., Chang, L., Klein, W.L., Van Duyne, R.P., 2005. J. Am. Chem. Soc. 127 (7), 2264–2271.
Haes, A.J., Hall, W.P., Chang, L., Klein, W.L., Van Duyne, R.P., 2004. Nano Lett. 4 (6), 1029–1034.
Hamley, I.W., 2012. The amyloid beta peptide: a chemist's perspective. Chem. Rev. 112 (10), 5147–5192.
Hegnerová, K., Bockova, M., Vaisocherová, H., Krištofiková, Z., Říčný, J., Řípová, D., Homola, J., 2009. Sens. Actuators B 139 (1), 69–73.
Hung, V.W.-S., Masoom, H., Kerman, K., 2012. J. Electroanal. Chem. 681, 89–95.
Hung, V.W.S., Cheng, X.R., Li, N., Veloso, A.J., Kerman, K., 2013. J. Electrochem. Soc. 160 (7), G3097–G3101.
Jaruszewski, K.M., Curran, G.L., Swaminathan, S.K., Rosenberg, J.T., Grant, S.C., Ramakrishnan, S., Lowe, V.J., Poduslo, J.F., Kandimalla, K.K., 2014. Biomaterials 35 (6), 1967–1976.
Kaminski Schierle, G.S., Bertoncini, C.W., Chan, F.T., van der Goot, A.T., Schwedler, S., Skepper, J., Schlachter, S., van Ham, T., Esposito, A., Kumita, J.R., Nollen, E.A., Dobson, C.M., Kaminski, C.F., 2011. Chemphyschem 12 (3), 673–680.
Kang, M.K., Lee, J., Nguyen, A.H., Sim, S.J., 2015. Biosens. Bioelectron. 72, 197–204.
Kaushik, A., Solanki, P.R., Kaneto, K., Kim, C., Ahmad, S., Malhotra, B.D., 2010. Electroanalysis 22 (10), 1045–1055.
Kaushik, A., Vasudev, A., Arya, S.K., Pasha, S.K., Bhansali, S., 2014. Biosens. Bioelectron. 53, 499–512.
Kaushik, A., Yndart, A., Jayant, R.D., Sagar, V., Atluri, V., Bhansali, S., Nair, M., 2015. Int. J. Nanomed. 10, 677.
Kolarova, M., García-Sierra, F., Bartos, A., Ricny, J., Ripova, D., 2012. Int. J. Alzheimer's Dis., ID: 731526
Kumar, S.T., Meinhardt, J., Fuchs, A.-K., Aumüller, T., Leppert, Jr, Büchele, B., Knüpfer, U., Ramachandran, R., Yadav, J.K., Prell, E., 2014. ACS Nano 8 (11), 11042–11052.
Kurapati, K.R.V., Samikkannu, T., Atluri, V.S.R., Kaftanovskaya, E., Yndart, A., Nair, M. P., 2014. PLoS One 9 (11), e112818.
LaFerla, F.M., Green, K.N., Oddo, S., 2007. Nat. Rev. Neurosci. 8 (7), 499–509.
Laske, C., Sohrabi, H.R., Frost, S.M., López-de-Ipiña, K., Garrard, P., Buscema, M., Dauwels, J., Soekadar, S.R., Mueller, S., Linnemann, C., 2015. Alzheimer's Dementia 11 (5), 561–578.
Lee, Y.K., Lee, K.S., Kim, W.M., Sohn, Y.S., 2014. PLoS One 9 (6), e98992.
Li, H., Cao, Y., Wu, X., Ye, Z., Li, G., 2012. Talanta 93, 358–363.
Lien, T.T.N., Takamura, Y., Tamiya, E., Vestergaard, Md.C., 2015. Anal. Chim. Acta 892 (10), 69–76.
Liu, L., He, Q., Zhao, F., Xia, N., Liu, H., Li, S., Liu, R., Zhang, H., 2014. Biosens. Bioelectron. 51, 208–212.
Liu, L., Xia, N., Jiang, M., Huang, N., Guo, S., Li, S., Zhang, S., 2015. J. Electroanal. Chem. 754, 40–45.
Liu, L., Zhao, F., Ma, F., Zhang, L., Yang, S., Xia, N., 2013. Biosens. Bioelectron. 49, 231–235.
Luongo, K., Holton, A., Kaushik, A., Spence, P., Ng, B., 2013. Biomicrofluidics 7 (3), 034108.
Martić, S., Beheshti, S., Kraatz, H.B., Litchfield, D.W., 2012a. Chem. Biodivers. 9 (9), 1693–1702.
Martić, S., Beheshti, S., Rains, M.K., Kraatz, H.-B., 2012b. Analyst 137 (9), 2042–2046.
Martic, S., Rains, M.K., Kraatz, H.-B., 2013. Anal. Biochem. 442 (2), 130–137.
Mosconi, L., Brys, M., Glodzik-Sobanska, L., De Santi, S., Rusinek, H., de Leon, M.J., 2007. Exp. Gerontol. 42 (1), 129–138.
Mount, C., Downton, C., 2006. Nat. Med. 12 (7), 780–784.
Nestor, P.J., Scheltens, P., Hodges, J.R., 2004. Nature, S34–S41.
Oh, J., Yoo, G., Chang, Y.W., Kim, H.J., Jose, J., Kim, E., Pyun, J.C., Yoo, K.H., 2013. Biosens. Bioelectron. 50, 345–350.
Pasha, S.K., Kaushik, A., Vasudev, A., Snipes, S.A., Bhansali, S., 2014. J. Electrochem. Soc. 161 (2), B3077–B3082.
Rains, M.K., Martić, S., Freeman, D., Kraatz, H.B., 2013. ACS Chem. Neurosci. 4; , pp. 1194–1203.
Rama, E.C., González-García, M.B., Costa-García, A., 2014. Sens. Actuators B 201, 567–571.
Raymond, S.B., Treat, L.H., Dewey, J.D., McDannold, N.J., Hynynen, K., Bacskai, B.J., 2008. PLoS One 3 (5), e2175.
Rushworth, J.V., Ahmed, A., Griffiths, H.H., Pollock, N.M., Hooper, N.M., Millner, P.A., 2014. Biosens. Bioelectron. 56, 83–90.
Schenk, D., Barbour, R., Dunn, W., Gordon, G., Grajeda, H., Guido, T., Hu, K., Huang, J., Johnson-Wood, K., Khan, K., 1999. Nature 400 (6740), 173–177.
Sehgal, N., Gupta, A., Valli, R.K., Joshi, S.D., Mills, J.T., Hamel, E., Khanna, P., Jain, S.C., Thakur, S.S., Ravindranath, V., 2012. Proc. Natl Acad. Sci. 109 (9), 3510–3515.
Shah, P., Kaushik, A., Zhu, X., Zhang, C., Li, C.-Z., 2014. Analyst 139 (9), 2088–2098.
Shapshak, P., Rodriguez, H.E., Kayathri, R., Levine, A., Chiappelli, F., Minagar, A., 2008. Bioinformation 2 (8), 348–357.
Shaw, L.M., Vanderstichele, H., Knapik-Czajka, M., Clark, C.M., Aisen, P.S., Petersen, R.C., Blennow, K., Soares, H., Simon, A., Lewczuk, P., 2009. Ann. Neurol. 65 (4), 403–413.
Shin, K.-S., Kim, M.J., Lee, S.H., Kang, J.Y., 2015. In: 28th IEEE International Conferene, pp. 604–607. IEEE.
Simioni, S., Cavassini, M., Annoni, J.-M., Abraham, A.R., Bourquin, I., Schiffer, V., Calmy, A., Chave, J.-P., Giacobini, E., Hirschel, B., 2010. Aids 24 (9), 1243–1250.
Sjögren, M., Andreasen, N., Blennow, K., 2003. Clin. Chim. Acta 332 (1), 1–10.
Tsitsopoulos, P.P., Marklund, N., 2013. Front. Neurol. 4 (79), 1–17.
Veloso, A.J., Chow, A.M., Ganesh, H.V.S., Li, N., Dhar, D., Wu, D.C.H., Mikhaylichenko, S., Brown, I.R., Kerman, K., 2014. Anal. Chem. 86 (10), 4901–4909.
Veloso, A.J., Kerman, K., 2012. Bioelectrochemistry 84, 49–52.
Verdile, G., Fuller, S., Atwood, C.S., Laws, S.M., Gandy, S.E., Martins, R.N., 2004. Pharmacol. Res. 50 (4), 397–409.
Vestergaard, Md, Kerman, K., Saito, M., Nagatani, N., Takamura, Y., Tamiya, E., 2005. J. Am. Chem. Soc. 127 (34), 11892–11893.
Viola, K.L., Sbarboro, J., Sureka, R., De, M., Bicca, M.A., Wang, J., Vasavada, S., Satpathy, S., Wu, S., Joshi, H., 2015. Nat. Nanotechnol. 10 (1), 91–98.
Wadghiri, Y.Z., Sigurdsson, E.M., Sadowski, M., Elliott, J.I., Li, Y., Scholtzova, H., Tang, C.Y., Aguinaldo, G., Pappolla, M., Duff, K., 2003. Mag. Reson. Med. 50 (2), 293–302.
Wolfe, M.S., 2001. J. Med. Chem. 44 (13), 2039–2060.
Wu, C.-C., Ku, B.-C., Ko, C.-H., Chiu, C.-C., Wang, G.-J., Yang, Y.-H., Wu, S.-J., 2014. Electrochim. Acta 134, 249–257.
Xia, N., Zhang, Y., Guan, P., Hao, Y., Liu, L., 2015. Sens. Actuators B 213, 111–115.
Xu, Y., Wang, D., Luo, Y., Li, W., Shan, Y., Tan, X., Zhu, C., 2015. Neurobiol. Aging 36 (1), 157–168.
Yang, L.-B., Lindholm, K., Yan, R., Citron, M., Xia, W., Yang, X.-L., Beach, T., Sue, L., Wong, P., Price, D., 2003. Nat. Med. 9 (1), 3–4.
Yu, Y., Sun, X., Tang, D., Li, C., Zhang, L., Nie, D., Yin, X., Shi, G., 2015. Biosens. Bioelectron. 68, 115–121.
Zhang, L., Kai, T., Sun, Z., Hao, Y., Tu, Q., Zhou, F., 2013a. Electroanalysis 25 (7), 1659–1664.
Zhang, X., Tian, Y., Li, Z., Tian, X., Sun, H., Liu, H., Moore, A., Ran, C., 2013b. J. Am. Chem. Soc. 135 (44), 16397–16409.
Zhang, X., Tian, Y., Zhang, C., Tian, X., Ross, A.W., Moir, R.D., Sun, H., Tanzi, R.E., Moore, A., Ran, C., 2015. Proc. Natl. Acad. Sci. 112 (31), 9734–9739.
Zhao, Z., Zhu, L., Bu, X., Ma, H., Yang, S., Yang, Y., Hu, Z., 2015. Chem. Commun. 51 (4), 718–721.